

**ESTIMATION OF THE RATE OF CAPILLARY RISE IN
SAND AND SANDY LOAM BASED ON ONE
DIMENSIONAL SOIL COLUMN**

Htet Htet Aung

**A Thesis Submitted in Partial Fulfillment of the Requirements for the
Degree of Master of Engineering in Civil Engineering
Suranaree University of Technology
Academic Year 2012**

การประมาณค่าอัตราการเพิ่มขึ้นของคาพิวลาเรียในดินทราย
และดินร่วนปนทราย เพื่อประยุกต์ใช้ในการควบคุม
ความเค็มในดินที่มีการเคลื่อนที่แบบ 1 มิติ

นางแซท แซท อัง

วิทยานิพนธ์นี้เป็นส่วนหนึ่งของการศึกษาตามหลักสูตรปริญญาวิศวกรรมศาสตรมหาบัณฑิต
สาขาวิชาวิศวกรรมโยธา
มหาวิทยาลัยเทคโนโลยีสุรนารี
ปีการศึกษา 2555

**ESTIMATION OF THE RATE OF CAPILLARY RISE IN SAND
AND SANDY LOAM BASED ON ONE DIMENSIONAL
SOIL COLUMN**

Suranaree University of Technology has approved this thesis submitted in partial fulfillment of the requirements for a Master's Degree.

Thesis Examining Committee

(Prof. Dr. Suksun Horpibulsuk)

Chairperson

(Asst. Prof. Dr.Chatchai Jothityangkoon)

Member (Thesis Advisor)

(Assoc. Prof. Dr.Avirut Chinkulkijniwat)

Member

(Prof. Dr. Sukit Limpijumnong)

Vice Rector for Academic Affairs

(Assoc.Prof.Flt.Lt.Dr.Kontorn Chamniprasart)

Dean of Institute of Engineering

แชน แชน อัง : การประมาณค่าอัตราการเพิ่มขึ้นของคาพิลลารีในดินทราย
และดินร่วนปนทราย เพื่อประยุกต์ใช้ในการควบคุมความเค็มในดินที่มีการเคลื่อนที่
แบบ 1 มิติ (ESTIMATION OF THE RATE OF CAPILLARY RISE IN SAND AND
SANDY LOAM BASED ON ONE DIMENSIONAL SOIL COLUMN) อาจารย์ที่ปรึกษา
: ผู้ช่วยศาสตราจารย์ ดร.ฉัตรชัย โชติษฐยางกูร, 95 หน้า

ดินเค็มเป็นปัญหาสิ่งแวดล้อมที่มีความสำคัญ มีผลต่อการใช้ประโยชน์ที่ดินทั้งในประเทศที่
พัฒนาแล้ว และประเทศที่กำลังพัฒนา การแก้ปัญหาดินเค็มวิธีหนึ่งทำได้โดยการควบคุมการเกิดการ
เพิ่มขึ้นของความสูงคาพิลลารี ของการไหลของน้ำใต้ดินเค็ม เป้าหมายของการศึกษานี้มุ่งหาวิธีอย่าง
ง่ายในการประมาณอัตราการเพิ่มขึ้นของความสูงคาพิลลารีในดินที่ไม่อิ่มตัวด้วยน้ำ โดยใช้การหา
ผลลัพธ์ด้วยการวิเคราะห์ จากสมการเทอร์ซาคี และการหาผลลัพธ์ด้วยวิธีเชิงตัวเลขจากสมการของ
ริชาร์ด ผลการประมาณอัตราการเพิ่มขึ้นของความสูงคาพิลลารีทั้งดินทรายและดินร่วนปนทราย ถูก
นำมาเปรียบเทียบกับผลจากการทดลอง แบบจำลองการเคลื่อนที่แนวตั้งแบบไม่อิ่มตัวด้วยน้ำ ได้ถูก
พัฒนาบนพื้นฐานของสมการริชาร์ดสำหรับการไหลคาพิลลารี 1 มิติ พารามิเตอร์สำหรับแบบจำลอง
ประมาณได้จากกราฟที่สอดคล้องกันระหว่างผลจากการจำลอง และผลการทดลอง โดยใช้วิธี
ย้อนกลับ การประมาณความสูงคาพิลลารีสูงสุด และอัตราการเพิ่มขึ้นของความสูงคาพิลลารีได้
ผลลัพธ์ที่ดี ทั้งกรณีใช้การหาผลลัพธ์ด้วยการวิเคราะห์ และการจำลองวิธีเชิงตัวเลข อย่างไรก็ตาม
แบบจำลองเหล่านี้ยังไม่สามารถอธิบายความแปรเปลี่ยนของความชื้นของดินตามค่าระดับความสูง
ของแท่งดินได้อย่างสมบูรณ์

สาขาวิชา วิศวกรรมโยธา
ปีการศึกษา 2555

ลายมือชื่อนักศึกษา _____
ลายมือชื่ออาจารย์ที่ปรึกษา _____

HTET HTET AUNG : ESTIMATION OF THE RATE OF CAPILLARY
RISE IN SAND AND SANDY LOAM BASED ON ONE DIMENSIONAL
SOIL COLUMN. THESIS ADVISOR : ASST. PROF. CHATCHAI
JOTHITYANGKOON, Ph.D., 95 PP.

UNSATURATED SOILS/TERZAGHI'S EQUATION/RICHARDS EQUATION
ANALYTICAL SOLUTION/NUMERICAL SOLUTION/ REVERSE METHOD

Soil salinity is one of the main environmental problems affecting extensive areas of land in both developed and developing countries. This salinity problem can be solved by capillary rise control of saline groundwater flow. The aim is to find a simple way to estimate the rate of capillary rise in the unsaturated soils using analytical solution based on Terzaghi's equation and numerical solution based on Richards equation. Estimated rates of capillary rise of sand and sandy loam are compared with experimental results. The unsaturated upward movement model is developed based on Richards' equation for one dimensional capillary flow. Parameters for the model are estimated from fitted curve between simulate and experimental results using reversed method. Good estimation of maximum capillary height and the rate of capillary rise can be achieved by using analytical and numerical model. However, these models can not perfectly capture the variation of moisture content with different level of soil column.

School of Civil Engineering

Academic Year 2012

Student's Signature _____

Advisor's Signature _____

ACKNOWLEDGEMENT

I would like to express my sincere thanks to my thesis advisor, Assistant Professor Dr. Chatchai Jothityangkoon. He has been a steady influence throughout my master degree; he has oriented and supported me with promptness and care, and has always been patient and encouraging in times of new idea and difficulties; he has listened to my ideas and discussions with him frequently led to key insights. He has given the continuous encouragement that has helped me to complete this thesis successfully.

I also wish to express my deepest gratitude to my advisory committee members, Professor Dr. Suksun Horpiboonsuk and Associate Professor Dr. Avirut Chinkulkijniwat for their constructive comments, beneficial suggestions and productive advice to my research. And, I gratefully acknowledge all professors and all staffs in School of Civil Engineering School for their kind help.

Furthermore, I am very grateful to Miss Haruetai Maskong, Ph.D. student in School of Civil Engineering, for the use of her data based on experimental data and her support to complete my thesis.

I would also give my dearest thanks to Thailand International Development Cooperation Agency (TICA), Royal Thai Government for awarding this scholarship to me.

Likewise, I will also thank to Director General, Deputy Director General and departmental heads of Directorate of Water Resources and Improvement of River Systems for allowing and facilitating me to undertake this course. I also express my

sincere gratitude to sectional heads at Directorate of Water Resources and Improvement of River Systems for giving valuable advices during my study.

Finally, I most gratefully acknowledge my family and my friends for all their support throughout the period of this research.

Htet Htet Aung

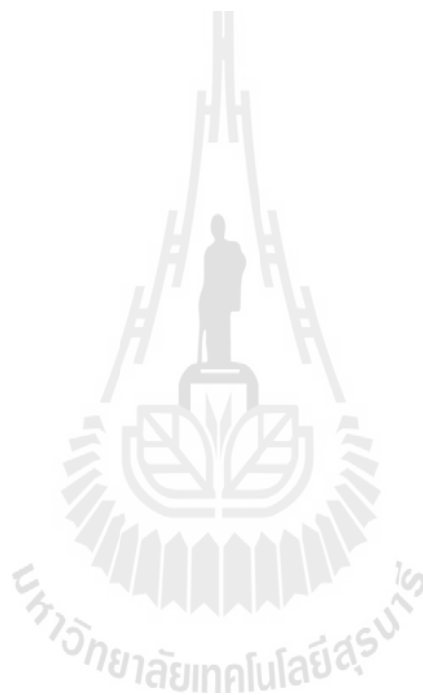


TABLE OF CONTENTS

	Page
ABSTRACT (THAI).....	I
ABSTRACT (ENGLISH).....	II
ACKNOWLEDGEMENTS.....	III
TABLE OF CONTENTS.....	V
LIST OF TABLES.....	VIII
LIST OF FIGURES.....	IX
SYMBOLS AND ABBREVIATIONS.....	XIII
CHAPTER	
I INTRODUCTION.....	1
1.1 General.....	1
1.2 Research Objective.....	2
1.3 Scope and limitation of study.....	2
II LITERATURE REVIEW.....	3
2.1 Salinity Affected Area.....	3
2.2 Physical Properties and Characteristics of Soils.....	4
2.2.1 Soil Texture.....	4
2.2.2 Porosity	5
2.2.3 Bulk Density.....	6
2.2.4 Soil Water Content.....	6

TABLE OF CONTENTS (Continued)

2.3	Unsaturated Soils.....	7
2.3.1	Total Soil Suction.....	8
2.3.2	Richard's Equation.....	9
2.3.3	Saturated Hydraulic Conductivity.....	10
2.3.4	Height of Capillary Rise.....	11
	(1) Capillary Rise in a Tube	11
	(2) Capillary Finger Model	13
2.4	Simplified Reverse Method.....	14
III	METHODOLOGY.....	17
3.1	Terzaghi's Equation for the Capillary Rise of Water in Soils.....	17
3.1.1	Analytical Solution.....	17
3.2	Richards Equation for the Capillary Rise of Water in Soils.....	22
3.2.1	Numerical Solution.....	22
IV	RESULTS AND DISCUSSIONS.....	28
4.1	Analysis of previous Experimental Results.....	28
4.2	Terzaghi's Equation for the Capillary Flow.....	30
4.2.1	Analytical Solution.....	30
4.3	Richards' Equation for the Capillary Flow.....	34
4.3.1	Numerical Solution for the Capillary Flow.....	34

TABLE OF CONTENTS (Continued)

(1) Numerical Solution for Sand	35
(2) Numerical Solution for Sandy loam	42
4.4 Estimation of Maximum Capillary Heights	45
4.5 Calibrated van Genuchten Parameters and Their Physical Properties.....	46
V CONCLUSIONS AND RECOMMENDATIONS.....	50
5.1 Conclusions.....	50
5.2 Recommendations.....	51
REFERENCES	52
APPENDICES	
APPENDIX A PREVIOUS EXPERIMENTAL DATA.....	55
APPENDIX B MATLAB CODES FOR ANALYTICAL SOLUTION BASED ON TERZAGHI'S EQUATION.....	67
APPENDIX C MATLAB CODES FOR NUMERICAL SOLUTION BASED ON RICHARDS EQUATION	75
APPENDIX D PUBLICATION	87
BIOGRAPHY	95

LIST OF TABLES

Table	Page
2.1 Typical value of saturated hydraulic conductivity based on texture and other properties (Smedema and Rycroft, 1983).....	11
4.1 The relation between capillary head and arrival time in sand soil column tests	29
4.2 The relation between capillary head and arrival time in sandy loam soil column tests.....	30
4.3 The calibrated van Genuchten parameters for each soil type and condition	46

LIST OF FIGURES

Figure	Page
2.1	Textural triangle showing a soil's textural class according to the percentage of sand, silt and clay it contains5
2.2	Unsaturated soils in the ground (Murray and Sivakumar, 2010)..8
2.3	Mechanical equilibrium for capillary rise in small diameter tube 13
2.4	Conceptual model for capillary rise and associated soil-water characteristic curve 14
2.5	Measured and fitted capillary flow for compacted soil station St 1 by proposed models 15
2.6	The resulting wetting SWCC of the van Genuchten (1980) Equations for loose and dense soil 16
3.1	System geometry for analytical prediction of rate of capillary rise 18
4.1	The capillary rise vs time for saline and non-saline sand (Column I and II) comparison between E.R of Maskong (2010) and A.S of Lu and Likos (2004) for $sh_c = 2$32
4.2	The capillary rise vs time for saline and non-saline sandy loam (Column III and IV) comparison between E.R of Maskong (2010) and A.S of Lu and Likos (2004) for $sh_c = 3.2$33
4.3	The capillary rise vs time for non-saline sand (Column I) comparison between E.R of Maskong (2010) and (2004) A.S of Lu and Likos using $sh_c = 2$ and 2.533

LIST OF FIGURES (Continued)

Figure	Page
4.4 The capillary rise vs time for saline sandy loam (Column IV) comparison between E.R of Maskong (2010) and (2004) A.S of Lu and Likos using $Sh_c = 3.2$ and 5	34
4.5 The relationship between capillary height and moisture content for Column I. Comparison of experimental and simulated results using numerical model applied van Genuchten (1980) equation with changing parameter a . (a) parameter $a = 0.011 \text{ cm}^{-1}$ (b) parameter $a = 0.03 \text{ cm}^{-1}$ (c) parameter $a = 0.012 \text{ cm}^{-1}$	37
4.6 The relationship between capillary height and moisture content for Column I. Comparison of experimental and simulated results using numerical model applied van Genuchten (1980) equation with changing parameter b . (a) parameter $b = 3$ (b) parameter $b = 6$ (c) parameter $b = 5$	39
4.7 The relationship between capillary height and moisture content for Column I. Comparison of experimental and simulated results using numerical model applied van Genuchten (1980) equation with changing parameter K_s . (a) parameter $K_s = 120 \text{ cm/d}$ (b) parameter $K_s = 180 \text{ cm/d}$ (c) parameter $K_s = 150 \text{ cm/d}$	41

LIST OF FIGURES (Continued)

Figure	Page
4.8 The relationship between capillary height and moisture content for Column II. Comparison of experimental and simulated results using numerical model applied van Genuchten (1980) equation with $a = 0.02 \text{ cm}^{-1}$, $b = 5$ and $K_s = 150 \text{ cm/d}$	42
4.9 The relationship between capillary height and moisture content for Column III. Comparison of experimental and simulated results using numerical model applied van Genuchten (1980) equation with $a = 0.01 \text{ cm}^{-1}$, $b = 3.6$ and $K_s = 3 \text{ cm/d}$ with constant bottom moisture content.....	43
4.10 The relationship between capillary height and moisture content for Column III. Comparison of experimental and simulated results using numerical model applied van Genuchten (1980) equation with $a = 0.01 \text{ cm}^{-1}$, $b = 3.6$ and $K_s = 3 \text{ cm/d}$ with decreasing bottom moisture content with time.....	44
4.11 The relationship between capillary height and moisture content for Column IV. Comparison of experimental and simulated results using numerical model applied van Genuchten (1980) equation with $a = 0.01 \text{ cm}^{-1}$, $b = 3.9$ and $K_s = 3 \text{ cm/d}$ with decreasing bottom moisture content with time.....	45
4.12 The resulting SWCCs of the van Genuchten (1980) equation for saline soils. (a) for sand (b) for sandy loam.	48

LIST OF FIGURES (Continued)

Figure	Page
4.13 The capillary rise vs time saline sand (Column II) comparison between E.R of Maskong (2010) and A.S of Lu and Likos (2004) using $S=I/h_a$	48
4.14 The capillary rise vs time for non-saline sandy loam (Column III) Comparison between E.R of Maskong (2010) and A.S of Lu and Likos (2004) using $S=I/h_a$	49
4.15 The capillary rise vs time for saline sandy loam (Column IV) Comparison between E.R of Maskong (2010) and A.S of Lu and Likos (2004) using $S=I/h_a$	49

CHAPTER I

INTRODUCTION

1.1 General

The expansion of salinity-affected area in Northeast region of Thailand has been a serious environmental problem that cause to the decreasing of agricultural productivity and food production in this region. It is estimated that an area of 6 million hectares, or 34 percent of arable land, is already affected by salt (Ghassemi, et al., 1995). Indications are that the problem is getting more widespread. A major cause of salt reaching the surface in this area is due to the rise of saline watertables to the capillary fringe and consequently the rise of salt to the surface (Konyai, et al., 2009; Loffler and Kubiniok, 1988). Upward movement of these saline waters contributes to the salinisation of the area.

Capillary rise is the upward flux of water from water table, which is driven by capillary forces in the soil's pore spaces. At the water table, soil is saturated and water is at atmospheric pressure. The capillary pressure head (soil matric potential) is a function of soil moisture content, and increases as soil moisture decreases. If the soil above the water table is not saturated, a soil matric potential gradient exists that induces an upward moisture flux from the water table.

Three fundamental physical characteristics related to capillary rise are of primary practical concern: (1) the maximum height of capillary rise, (2) the fluid storage capacity of capillary rise, and (3) the rate of capillary rise. Each of these aspects has an important influence on the overall engineering behavior of

unsaturated soil/water systems and is a complex function of both the soil and pore water properties. The aim is to find a simple way to estimate the rate of capillary rise in the unsaturated soils using analytical solution based on Terzaghi's equation and numerical solution based on Richards equation. These solutions will be simulated using MATLAB software version R2010a.

1.2 Research objectives

The main objectives of this study are as below:

- 1) to analyze the maximum capillary rise in sand and sandy loam of previous experimental results.
- 2) to estimate the rate of capillary rise in the unsaturated soils using analytical solution based on Terzaghi's equation and numerical solution based on Richards equation, and comparing to experimental data.
- 3) to identify the sensitive parameters influence on the estimation of capillary rise.

1.3 Scope and limitation of the study

In this study, the vertical movement of groundwater flow is only investigated. The practical predictions for the rate of capillary rise are presented in two types of soil which are sand and sandy loam. And, also the saline and non-saline water are used as the groundwater of the soils.

CHAPTER II

LITERATURE REVIEW

2.1 Salinity affected area

Soil salinity is one of the main environmental problems affecting extensive areas of land in both developed and developing countries.

For sub-humid region like the north-east of Thailand, saline soils are found cover an area of approximately 2.85 Mha. The source of the salt is primarily the dissolution of rock salt in the Mahasarakam Formation which underlies most of the Korat Plateau in North-east Thailand. Salt is released from saline rocks throughout the year, but it remains in the subsoil during the wet season and appears on the ground surface only during the dry season (Sinanuwong and Takaya, 1974). The rock salt beneath the moderately to the severely salt-affected areas is present at a depths range from 80 to 100 m. This salt can be dissolved with groundwater flow to be saline groundwater and moves to the soil surface with the capillary effect (Office of geology, 2005). Capillary suction in unsaturated soil above shallow water table can suck soil moisture with salinity to store in its voids (Fredlund and Rahardjo, 1993).

Arunin (1987) has shown that the reason for the spread of salinisation is primarily the removal of forest cover leading to increased groundwater recharge. The groundwater recharge on deforested uplands allows deep groundwater flow systems to dissolve and transport the salt towards lowland discharge areas. Another source of salt is the shallow interflow in the regolith forming local flow systems. As salinity increases, more salts will appear at the soil surface.

2.2 Physical properties and characteristics of soils

2.2.1 Soil Texture

Soil texture refers to the relative proportion of sand, silt and clay size particles in a sample of soil. The soil texture triangle in Figure 2.1 depicts the various texture classes. A soil can be assigned based upon the size fraction ratios. Clay size particles are the smallest being less than 0.002 mm in size. Silt is a medium size particle falling between 0.002 and 0.05 mm in size. The largest particle is sand with diameters between 0.05 for fine sand to 2.0 mm for very coarse sand. Use of the triangle is fairly straightforward. Soils that are dominated by clay are called fine textured soils while those dominated by larger particles are referred to as coarse textured soils.

Examination of the texture triangle shows that finer soils (clays) are located at the top of the triangle, coarser soils (sands) in the lower left corner, and intermediate soils (silts) in the lower right corner. The centre of the triangle is composed of clay loam and loam soil types. These two soil types, especially the clay loam, have an even ratio of fine, intermediate and coarse size fractions. Their infiltration rates, CEC, specific surface area, and other physical characteristics will be between those soils that border them on either side, that is, a clay loam will conduct more water than a silty clay loam, but less than a sandy clay loam (Tindall, et al., 1999). Agriculturally, this clay loam would be a preferable medium under most circumstances, because it would retain more moisture and have better aeration and drainage than other soils, and would also have an ample nutrient supply.



Figure 2.1 Textural triangle showing a soil's textural class according to the percentage of sand, silt and clay it contains.

2.2.2 Porosity

Soils are composed of mixtures of discrete large and small particles that may be loose single grains or bound in the form of aggregates, but the quantity of smaller particles and the aggregate size within a given soil has a marked effect on porosity. Porosity is expressed as a volume percent, ranging in most soils from 30-60%. Generally, the smaller the particle size the smaller the pores, but the greater the porosity. Hence, coarse soils have a lower porosity than fine soils. However, particle sorting also has an effect, so this tendency is not absolute.

Porosity (n) is expressed by

$$n = \frac{V_v}{V_t} \quad (2.1)$$

where, V_v is the volume of void-space (such as fluids) and V_t is the total or bulk volume of material, including the solid and void components.

2.2.3 Bulk density

The bulk density of a porous media is usually expressed in terms of dry soil, and is the ratio of media mass to total volume. Since the volume fraction is defined as a ratio of the volume of a phase to the total volume of media, the sum of the ratios of all phases represents that total volume and, thus, equal 1. Dry bulk density (ρ_b) is calculated as follows:

$$\rho_b = \frac{M_s}{V_t} \quad (2.2)$$

where M_s is dry mass of porous media.

2.2.4 Soil water content

The water content in soils on a mass basis, w , is defined as the ratio of the mass of the water, M_w , in the given soil sample to the mass of the solid material, M_s . And, the water content, w , is also referred to as the gravimetric water content. It is presented as a percentage (i.e., w (%)):

$$w = \frac{M_w}{M_s} \times 100 \quad (2.3)$$

The volumetric soil moisture content (or simply soil moisture content) of a soil (θ_v) is defined as the ratio of the volume of water, V_w , to the total volume of soil V_t ,

$$\theta_v = \frac{V_w}{V_t} \times 100 \quad (2.4)$$

Also, the volumetric moisture content can be expressed in terms of the mass-basis water content, w , according to the following formula:

$$v_w = w \frac{\rho_b}{\rho_w} \times 100 \quad (2.5)$$

where, ρ_b is the bulk density of the soil and ρ_w is the water density.

2.3 Unsaturated soils

The term soil as used in geotechnical engineering encompasses a wide spectrum of particulate materials. In the saturated state all the void spaces between the particles are filled with water, but in the unsaturated state a proportion of void spaces is filled with air. The solid particles, water and air are the phases making up a soil mass. Interpretation of the behavior of unsaturated soils requires the differences in the air and water pressures, the phase compressibilities and their interactions, as well as chemical effects, to be taken into account.

Around one-third of earth's surface is situated in arid or semi-arid regions where the potential evaporation exceeds the precipitation. However, any soil near the ground surface in a relatively dry environment is liable to have a negative pore water pressure (water pressure relative to a datum of atmospheric air pressure) and could experience de-saturation on air entry into the pore spaces. Though the soil may be saturated for some height above the water table, if the pore water pressure drops sufficiently, air will enter the pore spaces. Figure 2.2 illustrates the change from a positive pore water pressure below the water table to negative pore water pressure above the water table. Negative pore water pressure is the key to understanding

unsaturated soil behavior and in interpreting the significance to engineering structures (Murray and Sivakumar, 2010).

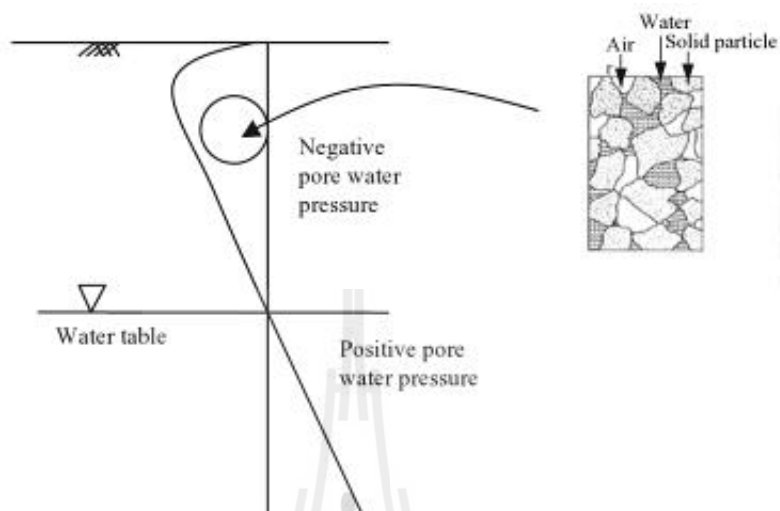


Figure 2.2 Unsaturated soils in the ground (Murray and Sivakumar, 2010).

2.3.1 Total soil suction

Total soil suction quantifies the thermodynamic potential of soil pore water relative to a reference potential of free water. Free water in this regard is defined as water containing no dissolved solutes, having no interactions with other phases that impart curvature to the air-water interface, and having no external forces other than gravity. The total suction, \mathcal{E} , of a soil is made up of two components, namely, the matric suction, and the osmotic suction:

$$\mathcal{E} = (u_a - u_w) + f \quad (2.6)$$

where, $(u_a - u_w)$ is matric suction, u_a is the pore-air pressure, u_w is the pore-water pressure and f is the osmotic suction.

Matric suction is intended to describe the component of suction arising from interactions between the pore water and the soil solids. Suction arising from the presence of dissolved solutes is referred to as osmotic suction. The van't Hoff equation states that the osmotic pressure of a solution depends on the concentration of osmotically active solute particles. The concentration of solute particles is converted to a pressure by multiplying it by the gas constant and the absolute temperature. The following formula:

$$f = gMRT \quad (2.7)$$

where, f is the osmotic pressure (atm), g is the number of particles / mol in solution, M is the concentration (mmol/L), R is the gas constant (0.082 L.atm/mol.K) and T is the absolute temperature (°K).

2.3.2 Richard's equation

Darcy's Law for unsaturated soils may be written as

$$q_x = -K_x(\theta) \frac{\partial H}{\partial x}, \quad q_y = -K_y(\theta) \frac{\partial H}{\partial y}, \quad q_z = -K_z(\theta) \frac{\partial H}{\partial z} \quad (2.8)$$

where, q_x , q_y , q_z are the soil-water fluxes in the x, y and z directions, respectively, $K(\theta)$ is the hydraulic conductivity and H is the the hydraulic head.

Conservation of mass says the rate of change of saturation in a closed volume is equal to the rate of change of the total sum of fluxes into (q_{in}) and out (q_{out}) of that volume, put in mathematical language:

$$\frac{\partial \theta}{\partial t} = \nabla \left(\sum_{i=1}^n q_{in} - \sum_{i=1}^n q_{out} \right) \quad (2.9)$$

where, ∇ is the differential operator, θ is the water content, and t is time.

Put in the one dimensional form for the vertical direction

$$\frac{\partial \theta}{\partial t} = - \frac{\partial q}{\partial z} \quad (2.10)$$

Substituting q from equation (2.8) in the equation (2.10),

$$\frac{\partial \theta}{\partial t} = \frac{\partial}{\partial z} \left[K \left(\frac{\partial H}{\partial z} \right) \right] \quad (2.11)$$

Substituting for $H = h + z$: (where, h is matric suction head)

$$\frac{\partial \theta}{\partial t} = \frac{\partial}{\partial z} \left[K \left(\frac{\partial h_m}{\partial z} + \frac{\partial z}{\partial z} \right) \right] = \frac{\partial}{\partial z} \left[K \left(\frac{\partial h_m}{\partial z} + 1 \right) \right] \quad (2.12)$$

The above equation is known commonly as Richard's equation which represents the movement of water in unsaturated soils, and was formulated by Richards (1931). It is a non-linear partial differential equation.

2.3.3 Saturated hydraulic conductivity

Hydraulic conductivity, mathematically represented as K , is a property of soil or rock, in the groundwater, that describes the ease with which water can move through pore spaces or fractures. It depends on the intrinsic permeability of the material and on the degree of saturation. Saturated hydraulic conductivity, K_s , describes water movement through specific saturated soil and is relatively constant.

Table 2.1 Typical value of saturated hydraulic conductivity based on texture and other soil properties (Smedema and Rycroft, 1983)

Soil properties	Order of magnitude of saturated hydraulic conductivity (m/d)
Coarse gravelly sand	10 – 50
Medium sand	1 – 5
Sandy loam/fine sand	1 – 3
Loam/clay loam/clay, well structured	0.5 – 2
Very fine sandy loam	0.2 - 0.5
Clay loam/clay,poorly structured	0.02 - 0.2
Dense clay, not cracked, no biopores	<0.002

The values will also depend on the type of clay mineral present in fine-textured soils and on the presence of root channels and holes made by earthworms.

2.3.4 Height of capillary rise

(1) Capillary rise in a tube

Capillary rise in soil describes the upward movement of water above the water table resulting from the gradient in the water potential across the air-water interface at the wetting front. Capillary behavior can be analyzed by considering the surface tension, T_s , acting around the circumference of the meniscus. The surface tension, T_s , acts at an angle, τ , from the vertical. The angle is known as the contact angle, and its magnitude depends on the adhesion between the molecules in the contractile skin and the material comprising the tube (i.e., glass). Based on the

Young-Laplace Equation, to achieve mechanical equilibrium, the following relationship between the matric suction and the vertical force is valid at the interface:

$$u_a - u_w = T_s \cos \gamma \left(\frac{1}{r_1} + \frac{1}{r_2} \right) \quad (2.13)$$

In an ideal cylindrical capillary tube with a diameter d , $r_1 = r_2 = d/2$ and Eq. (2.13) becomes

$$u_a - u_w = \frac{4T_s \cos \gamma}{d} \quad (2.14)$$

A contact angle equal to zero describes a perfectly wetting material; 90° describes neutral wetting ability and an angle greater than 90° describes the interaction between water and a water repellent material. Consider the free body diagram in the area of the small dashed circle shown in Figure 2.3, to achieve mechanical equilibrium. Vertical force equilibrium considering $u_a - u_w$ acting over the area of meniscus and the vertical projection of T_s acting over the circumference of the meniscus leads to

$$(u_a - u_w) \frac{f}{4} d^2 = T_s f d \cos \gamma \quad (2.15)$$

which can be directly reduced to Eq. (2.14).

If the air pressure is set to a reference value of zero, water pressure has a negative value, representing a positive matric suction. The smaller the diameter of the capillary tube d , the greater the matric suction. The greater the wetting ability of the solid surface (i.e very small contact angle γ), the greater the matric suction.

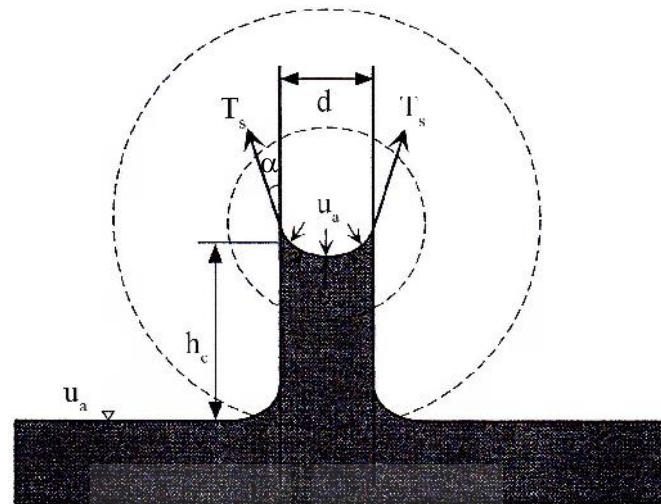


Figure 2.3 Mechanical equilibrium for capillary rise in small diameter tube.

The maximum height of capillary rise, h_c , can be evaluated by considering mechanical equilibrium in the area of the large dashed circle in Figure 2.3. Here, the total weight of the water column under the influence of gravity is balanced by surface tension along the water-solid interface as

$$h_c = \frac{4T_s \cos \alpha}{d \rho_w g} \quad (2.16)$$

where, g is the gravitational acceleration, and ρ_w is the density of water.

(2) Capillary finger model

The soil particles in the unsaturated zone are coated with layers of water. The void spaces between the soil particles are known as the soil pores. Below the water table the pore spaces are filled with water. Above the water table the pore spaces are filled with varied amounts of air and water.

As illustrated in the Figure 2.4, pore water rises above the water table under capillary suction. The soil remains essentially saturated, described by the saturated

water content θ_s , until the suction head reaches the air-entry head, designated h_a . The air-entry head may be defined as the suction head at which air initially begins to displace water from the soil pores.

The saturated zone extending from the water table up to the air-entry head is commonly referred to as the capillary fringe. Above the air-entry head, the water content decreases with increasing height, reflecting the fact that fewer and smaller capillary fingers are present for a given cross section of the soil column with increasing elevation.

At the relatively large values of suction head, therefore, very little water is retained by the soil. The water content within this regime is commonly referred to as the residual water content, or θ_r .

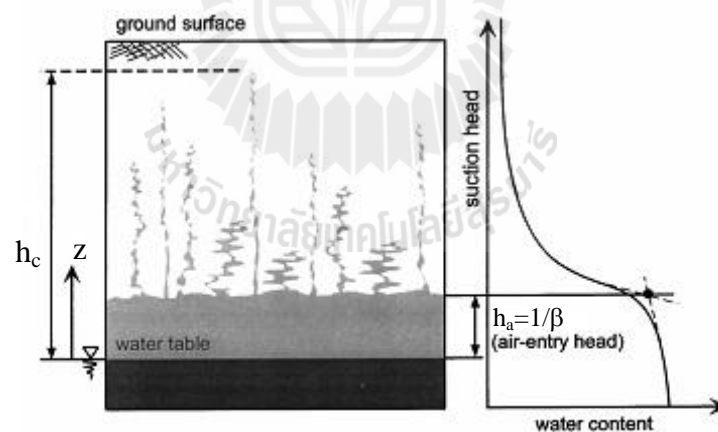


Figure 2.4 Conceptual model for capillary rise and associated soil-water characteristic curve.

2.4 Simplified reverse method

Jitrapinate et al. (2011) developed the simplified method for determining the unsaturated hydraulic conductivity $K(\theta)$ and Soil Water Characteristic Curve (SWCC) for saline soils or soils directly in contact with saline water. Using a numerical solution of the Richards Equation to determine these parameters in an assumed form of the $K(\theta)$ function.

Based on inverse method, combination of measured flow under transient conditions and a numerical model are used to determine the value of parameters that produced the best fit between the model predictions and the observed cumulative capillary flow in dry soil columns. These estimated parameters are applied to predict the capillary flow using the HYDRUS-1D software version 4.14 and compare to this model. A sample solution of fitting curves of capillary flow with the data points and the resulting SWCC for saline soils are shown in Figures 2.5 and 2.6, respectively. In these figures, the measured data points are shown as symbols and the fitted curve as the lines.

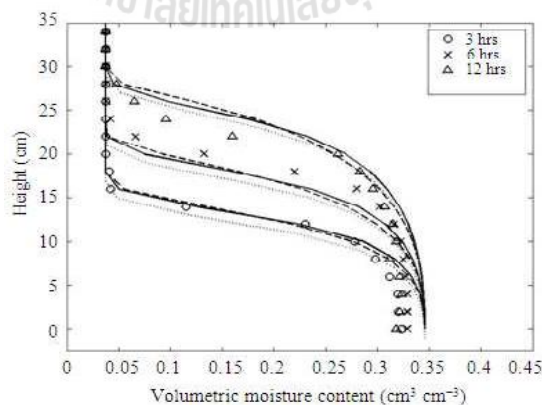


Figure 2.5 Measured and fitted capillary flow for compacted soil

station St1 by

proposed models.

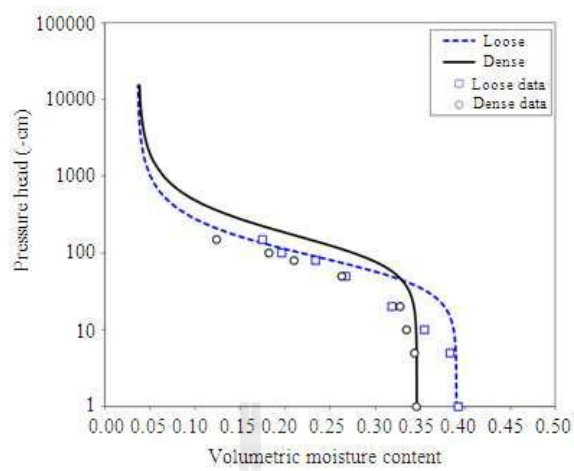
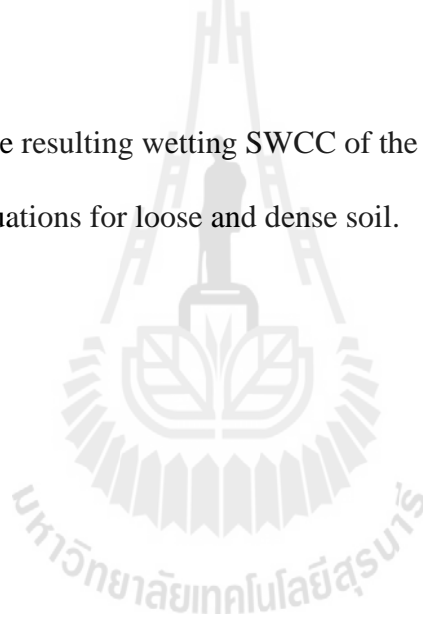


Figure 2.6 The resulting wetting SWCC of the van Genuchten (1980)

equations for loose and dense soil.



CHAPTER III

METHODOLOGY

3.1 Terzaghi's Equation for the capillary rise of water in soils

3.1.1 Analytical solution

Terzaghi (1943) formulated a simple theory based on Darcy's law and saturated hydraulic conductivity for predicting the rate of capillary rise in one – dimensional column of soil. To arrive at his solution for the rate of capillary rise, Terzaghi (1943) made two major assumptions: (1) that Darcy's law for saturated fluid flow is roughly applicable to unsaturated flow, and (2) that the hydraulic gradient i responsible for capillary rise (i.e., hydraulic gradient of the wetting front located at the elevation z) can be approximated as follows;

$$i = \frac{h_c - z}{z} \quad (3.1)$$

where, h_c is the maximum height of capillary rise; and z is distance measured positive upward from the elevation of the water table (Figure 3.1). Physically, h_c represents the drop in pressure head across the air–water interface at the wetting front in the soil pores.

Terzaghi's other assumption, Darcy's law is valid for capillary rise, can be expressed in familiar mathematical terms as follows;

$$q = K_s i = n \frac{dz}{dt} \quad (3.2)$$

where, q is discharge velocity; K_s and n are the saturated hydraulic conductivity and porosity of the soil, respectively.

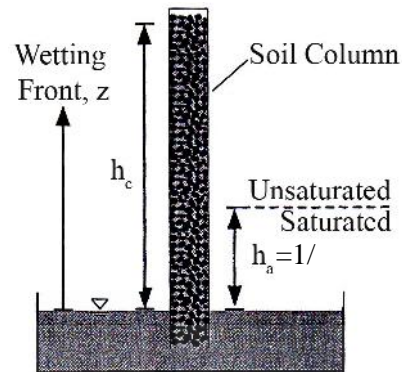


Figure 3.1 System geometry for analytical prediction of rate of capillary rise.

Solving Eqs. (3.1) and (3.2) and imposing an initial condition of zero capillary rise at zero time, Terzaghi arrived at the following solution describing the location of the capillary wetting front z as an implicit function of time;

$$t = n \frac{h_c}{K_s} \left(\ln \frac{h_c}{h_c - z} - \frac{z}{h_c} \right) \quad (3.3)$$

In reality, capillary rise above the air entry head is no longer governed by saturated hydraulic conductivity. The hydraulic conductivity of the unsaturated soil located above the air-entry head decreases dramatically as the pores begin to drain and the degree of saturation decreases with increasing rise. By the time the wetting front approaches h_c , the degree of saturation could be as low as a few percent and the hydraulic conductivity may be reduced by as much as 5–7 orders of magnitude its value at saturation. This significant reduction in hydraulic conductivity, together with the reduction in the available driving head ($h_c - z$), leads to a significant decrease in the rate of capillary rise as time progresses and the wetting front moves upward.

Lu and Likos (2004) developed a solution for the rate of capillary rise by incorporating Gardner's one-parameter exponential model Gardner (1958) to estimate the unsaturated hydraulic conductivity function. Gardner's model is expressed in terms of the saturated hydraulic conductivity K_s and suction head h as follows;

$$K = K_s \exp(Sh) \quad (3.4)$$

where, K is the unsaturated hydraulic conductivity at suction head h (cm) and S is a pore size distribution parameter (cm^{-1}) representing the rate of decrease in hydraulic conductivity with increasing suction head. The inverse of S has also been interpreted as the air-entry head, or equivalently, as the height of the saturated portion of the capillary fringe, i.e., $h_a = 1/S$.

Assuming Eq. (3.1) as the driving hydraulic gradient during capillary rise and Eq. (3.4) for the hydraulic conductivity at the wetting front z , the governing equation for one-dimensional capillary rise can be written as follows;

$$\frac{dz}{dt} = \frac{K_s}{n} \exp(-Sz) \left(\frac{h_c - z}{z} \right) \quad (3.5)$$

By Taylor's series expansion,

$$\exp(Sz) = \sum_{j=0}^m \frac{(Sz)^j}{j!} \quad (3.6)$$

Where the series index m goes to infinity. With Eq. (3.6), Eq. (3.5) becomes

$$\frac{\sum_{j=0}^m \frac{S^j z^{j+1}}{j!}}{h_c - z} dz = \sum_{j=0}^m \frac{S^j z^{j+1}}{j!(h_c - z)} dz = \frac{K_s}{n} dt \quad (3.7)$$

Integrating the above equation,

$$\int \sum_{j=0}^m \frac{S^j z^{j+1}}{j!(h_c - z)} dz = \sum_{j=0}^m \frac{S^j}{j!} \int \frac{z^{j+1}}{(h_c - z)} dz = \frac{K_s}{n} \int dt \quad (3.8)$$

From Gradshteyn et al., (1994), p. 69, we have a general form of integration

$$\begin{aligned} \int \frac{z^{j+1}}{(a+bz)} dz &= \frac{z^{j+1}}{(j+1)b} - \frac{az^j}{(j)b^2} + \frac{a^2 z^{j-1}}{(j-1)b^3} - \dots \\ &+ (-1)^j \frac{a^j z}{1 \cdot b^{j+1}} + (-1)^{j+1} \frac{a^{j+1}}{b^j} \ln(a+bz) \end{aligned} \quad (3.9)$$

From Eq. (3.8), let $a = h_c$, and $b = -1$ so that the above equation becomes

$$\begin{aligned} \int \frac{z^{j+1}}{(h_c - z)} dz &= \frac{z^{j+1}}{(j+1)(-1)} - \frac{h_c z^j}{(j)(-1)^2} + \frac{h_c^2 z^{j-1}}{(j-1)(-1)^3} - \dots \\ &+ (-1)^j \frac{h_c^j z}{1 \cdot (-1)^{j+1}} + (-1)^{j+1} \frac{h_c^{j+1}}{(-1)^j} \ln(h_c - z) \end{aligned} \quad (3.10)$$

The above equation can be rewritten in a compact form

$$\int \frac{z^{j+1}}{(h_c - z)} dz = - \sum_{s=0}^j \frac{h_c^s z^{j+1-s}}{j+1-s} - h_c^{j+1} \ln(h_c - z) \quad (3.11)$$

Substituting Eq. (3.11) back into Eq. (3.8),

$$\frac{K_s}{n} t + C = - \sum_{j=0}^m \frac{S^j}{j!} \left[\sum_{s=0}^j \frac{h_c^s z^{j+1-s}}{j+1-s} + h_c^{j+1} \ln(h_c - z) \right] \quad (3.12)$$

Consider the initial boundary condition is zero rise at time equal to zero,

$$\frac{K_s}{n} t = \sum_{j=0}^m \frac{S^j}{j!} \left[-\sum_{s=0}^j \frac{h_c^s z^{j+1-s}}{j+1-s} + h_c^{j+1} \ln \frac{h_c}{(h_c - z)} \right] \quad (3.13)$$

The simplified analytical solution can be written in series form as follows;

$$t = \frac{n}{K_s} \sum_j \frac{S^j}{j!} \left[h_c^{j+1} \ln \frac{h_c}{h_c - z} - \sum_{s=0}^j \frac{h_c^s z^{j+1-s}}{j+1-s} \right] \quad (3.14)$$

If the nonlinearity in hydraulic conductivity is ignored by setting the series index m to zero, Eq. (3.14) reduces to Terzaghi's original analytical solution Eq. (3.3). Convergent solutions are typically obtained by setting m equal to 10.

The material parameter S can be determined if either the hydraulic conductivity function or soil–water characteristic curve are known or estimated. Given the former, S can be determined in conjunction with Gardner's model to determine the “best fit” value. Given the latter, S can be determined using a graphical technique to estimate the air-entry head h_a and by recognizing that S may be interpreted as its inverse. The maximum height of capillary rise h_c may be approximated using a capillary tube analogy and applying the Young–Laplace equation to analyze mechanical equilibrium at the rising air/water interface. If both h_c and h_a are known, a dimensionless parameter Sh_c equal to h_c/h_a . For the wide range of soil tested ((Lane and Washburn, 1946); (Malik et al., 1989); and (Kumar and Malik, 1990)), the ratio h_c/h_a varies from 2 to 5 with only a few exceptions.

3.2 Richards Equation for the capillary rise of water in soils

3.2.1 Numerical solution

In virtually all studies of the unsaturated zone, the fluid motion is assumed to obey the classical Richards equation, which is obtained by applying the mass conservative law and the Darcy flow law (Bear, 1978; Hillel, 1980).

$$\frac{\partial n}{\partial t} = \frac{\partial}{\partial z} \left(K \frac{\partial h}{\partial z} \right) + \frac{\partial}{\partial z} K \quad (3.15)$$

where, t is the time and z is the vertical distance taken positive upward. If soil moisture content and pressure head h are uniquely related, then the left-hand side of Eq. (3.15) can be written

$$\frac{\partial n}{\partial t} = \frac{\partial n}{\partial h} \cdot \frac{\partial h}{\partial t}$$

which transforms Eq. (3.15) into

$$C \frac{\partial h}{\partial t} = \frac{\partial}{\partial z} \left[K \frac{\partial h}{\partial z} \right] + \frac{\partial}{\partial z} K \quad (3.16)$$

where, $C (= d_n/dh)$ is defined as the specific water capacity (i.e., the change in water content in a unit volume of soil per unit change in matric potential).

The constitutive relationship between K and h is known as the Soil Water Characteristic Curve and the Conductivity Function. In this study, the van Genuchten (1980) soil water characteristic function coupled with Mualem (1976) conductivity function was adopted. The model proposed by van Genuchten (1980) is as follows:

$$\theta = \theta_r + \frac{\theta_s - \theta_r}{[1 + (ah)^b]^c} \quad (3.17)$$

where θ is volumetric water content, θ_r and θ_s are the residual and saturated volumetric water contents, respectively, a is shape parameter (cm^{-1}), b and c are also shape parameters where c is $1-1/b$, and h is the pressure head (cm). van Genuchten (1980) derived the following conductivity function using Mualem (1976)'s model of conductivity:

$$K(\Theta) = K_s \Theta^{1/2} \left[1 - (1 - \Theta^{1/c})^c \right]^2 \quad (3.18)$$

where, K_s is the saturated hydraulic conductivity and Θ is the normalized volumetric water content $= (\theta - \theta_r) / (\theta_s - \theta_r)$.

As Eq. (3.16) is a non-linear partial differential equation, therefore in solving this equation, finite difference form has to be used. Different discretization schemes can be used using explicit or implicit methods. In the explicit method, a series of linearized independent equations is solved directly, while in the implicit method, a system of simultaneous linear algebraic equations (involving tridiagonal coefficient matrix with zero elements outside the diagonals) has to be solved. The partial differential equation is approximated by a finite difference equation replacing ∂t and ∂z by Δt and Δz respectively. A soil column is divided into many segments of equal length Δz and time is also divided by intervals of Δt . When Eq. (3.16) is solved by a finite difference technique choosing the implicit method, the Eq. (3.19) becomes

$$C_i^j \frac{h_i^{j+1} - h_i^j}{\Delta t} = \frac{1}{\Delta z} \left[K_{i+1/2}^j \left(\frac{h_{i+1}^{j+1} - h_i^{j+1}}{\Delta z} \right) - 1 \right] - \frac{1}{\Delta z} \left[K_{i-1/2}^j \left(\frac{h_i^{j+1} - h_{i-1}^{j+1}}{\Delta z} \right) - 1 \right] \quad (3.19)$$

where, the subscripts (i+1/2) and (i-1/2) of K mean that the values of K are evaluated at the midpoint between the nodes (i) and (i+1), and (i) and (i-1), respectively. The superscript j and (j+1) means that the preceding time step (t) and the prediction time step (t + Δt), respectively. (ie., i refers to the depth and j refers to time). Rearranging the terms in Eq. (3.10) to be

$$-F_3 h_{i-1}^{j+1} + (-F_2 + F_3 - F_1) h_i^{j+1} + F_2 h_{i+1}^{j+1} = -F_1 h_i^j - F_4 \quad (3.20)$$

where,

$$F_1 = \frac{C_i^j}{\Delta t}$$

$$F_2 = K_{i+1/2}^j = \frac{K_{i+1}^j + K_i^j}{2\Delta z^2}$$

$$F_3 = -K_{i-1/2}^j = \frac{K_i^j + K_{i-1}^j}{2\Delta z^2}$$

$$F_4 = \frac{K_{i+1}^j - K_{i-1}^j}{2\Delta z}$$

Let a = -F₃, b = (- F₂ + F₃ - F₁), c = F₂ and d = F₁h_i^j - F₄, and substituting these coefficients in Eq. (3.20) to set up general form of implicit method:

$$a h_{i-1}^{j+1} + b h_i^{j+1} + c h_{i+1}^{j+1} = d \quad (3.21)$$

When Eq. (3.21) is applied at all nodes, the result is a system of simultaneous linear algebraic equations with a tri-diagonal coefficient matrix with zero elements outside the diagonals and unknown values of h .

It was considered the problem of solving for equations above given the following initial and boundary conditions:

Dirichlet type (constant h or):

$$h(z,0) = h_{\text{initial}}, \quad 0 < z < L$$

$$h(0,t) = h_0, \quad t > 0$$

$$h(L,t) = h_{\text{initial}}, \quad t > 0$$

Neumann type (constant flux):

$$h(z,0) = h_{\text{initial}}, \quad z = 0$$

$$h(0,0) = h_0,$$

$$h(L,t) = h_{\text{initial}}, \quad t > 0$$

$$q(0,t) = q_0, \quad t > 0$$

Flux boundary condition (Neumann type)

For steady state flow, $\partial h / \partial t = 0$ and h is only a function of z , the most simple flow case is

$$\frac{d}{dz} \left[K \left(\frac{dh}{dz} + 1 \right) \right] = 0 \quad (3.22)$$

Integration of Eq. (3.22) yields:

$$K \left(\frac{dh}{dz} + 1 \right) = c \quad (3.23)$$

where, c is the integration constant, with $q = -c$. Rewriting yields

$$q = -K \left(\frac{dh}{dz} + 1 \right) = -c \quad (3.24)$$

For the last node,

$$\frac{dh}{dz} = \frac{c}{K} - 1 \quad (3.25)$$

$$\frac{h_{n+1} - h_n}{\Delta z} = \left(\frac{c}{K_{avg}} - 1 \right) \quad (3.26)$$

where,

$$K_{avg} = \frac{K_{n+1} + K_n}{2}$$

$$h_{n+1} = \left(\frac{c}{K_{avg}} - 1 \right) \Delta z + h_n \quad (3.27)$$

When Eq. (3.27) is written as Eq. (3.21) by changing n ;

$$ah_{n-1}^{j+1} + bh_n^{j+1} + ch_{n+1}^{j+1} = d \quad (3.28)$$

Substituting h_{n+1}

$$a_n h_{n-1}^{j+1} + b_n h_n^{j+1} + c_n \left[\left(\frac{c}{K_{avg}} - 1 \right) \Delta z + h_n \right] = d_n \quad (3.29)$$

$$a_n h_{n-1}^{j+1} + (b_n + c_n) h_n^{j+1} = d_n - c_n \left(\frac{c}{K_{avg}} - 1 \right) \Delta z \quad (3.30)$$

$$a_n h_{n-1}^{j+1} + (b_n + c_n) h_n^{j+1} = d_n + c_n \Delta z \left(1 + \frac{q}{K_{avg}} \right) \quad (3.31)$$

where, q is negative for infiltration (downward flow) and positive for evaporation (upward flow).



CHAPTER IV

RESULTS AND DISCUSSIONS

4.1 Analysis of previous experimental results

In order to examine the capillary rises, six uniform soil columns based on long column method from laboratory were studied. The long column method provided static equilibrium volumetric water content at selected elevation along an upright column of soil (Reynolds and Topp, 2008).

Similar to experimental set up for the long soil column suggested by (Reynolds and Topp, 2008), each column was 95 cm in depth and water content probes were installed at 10, 30, 50, 70, 90 cm from the column base, as the desired matric head values. Constant head device was used to keep constant head of inflow water at 10 cm from the column base, presented in Maskong (2010).

There were 2 types of soil sample (1) sand from sand pit at Pimai district Nakhon Ratchasima province, taking a sample with grain size passing sieve No.40 and retaining in sieve No.60, (2) sandy loam from Nong Khwao village, Non Thai district Nakhon Ratchasima province where facing soil salinity problem. Two types of groundwater were used for these experiments: (1) deionized (non-saline) water represented deionized groundwater (DG) and (2) saline water prepared by dissolving pure NaCl with water until becoming saturated saline water, represented saline groundwater (SG).

The experiments with six soil columns are:

- 1) Column I : Sand and DG (Non-saline sand)

- 2) Column II : Sand and SG (Saline sand)
- 3) Column III: Sandy loam and DG (Non-saline sandy loam)
- 4) Column IV: Sandy loam and SG (Saline sandy loam)
- 5) Column V : Sandy loam and SG adding artificial light
- 6) Column VI: Sandy loam and SG adding moisture at the soil surface. The experiments were described fully in Maskong (2010).

The experimental measurements of the moving and maximum height of capillary rise varied with time were observed and extracted to present in Table 4.1 and 4.2.

Table 4.1 shows the relation between capillary head and arrival time in sand soil column tests. For both SG and DG groundwater types in sand, the maximum capillary rise is 30 cm. The maximum capillary heights of sandy loam are 70 cm and 90 cm for the DG and SG types, respectively, that can be seen in Table 4.2.

Table 4.1 The relation between capillary head and arrival time in sand soil column tests

Capillary head (cm)	Column I		Column II	
	Moisture content (%)	Arrival Time (day)	Moisture content (%)	Arrival Time (day)
10	17.088	0.010	23.510	0.010
30	9.530	0.583	17.000	0.375
50	no change		no change	
70	no change		no change	
90	no change		no change	

Table 4.2 The relation between capillary head and arrival time in sandy loam soil column tests

Capillary head (cm)	Column III		Column IV and Column V	
	Moisture content (%)	Arrival Time (day)	Moisture content (%)	Arrival Time (day)
10	32.0	0.17	34.0	0.13
30	33.2	1.00	33.2	1.00
50	20.1	6.00	31.9	4.00
70	13.7	9.00	30.5	7.00
90	no change		19.2	12.00

Table 4.2 The relation between capillary head and arrival time in sandy loam soil column test (Continued)

Capillary head (cm)	Column VI	
	Moisture content (%)	Arrival Time (day)
10	36.1	0.17
30	no changes	
50	no changes	
70	no changes	
90	20.4	0.17

4.2 Terzaghi's equation for the capillary flow

4.2.1 Analytical solution

Rate of capillary rise for soil Column I to IV were predicted using Lu and Likos's analytical solution. There are three parameters such as $(1/h_a)$, K_s , and n .

Porosity (n) values of sand and sandy loam were 0.37 and 0.36, respectively, that are obtained from Maskong's (2010) experiments (seen in Appendix A). However, direct measurement of h_a and K_s were not available for soils. So, rate of capillary rises were firstly presented with the assuming required parameters that are taken from literatures. Next, the required parameters were predicted from numerical solutions using experimental data (Maskong, 2010), and then, rate of capillary rise of soils were evaluated with these predicted parameter values.

Direct measurement of h_a , K_s were not available for soils. K_s was taken from Table 2.1 and also, S to be used in Eq. (3.14) was assumed from Sh_c (h_c / h_a) (Lane and Washburn, 1946; Malik et al., 1989; and Kumar and Malik, 1990). And Sh_c was estimated in terms of "best fit" to the experimental data (Maskong, 2010) for the soils. Evaluating rate of capillary rise for the soils, the analytical solutions were solved using MATLAB software version R2010a code (seen in Appendix B).

Figure 4.1 shows the height of observed and simulated capillary rise as a function of time for Column I (non-saline sand) and Column II (saline sand). The analytical solutions (A.S) give a good fit to the experimental results (E.R) at the beginning period, time is about 15 mins. At the longer time, the rate of capillary rise of simulated results tends to decrease and take longer time to arrive maximum rise at about 0.3 m. The analytical solutions for both saline and non-saline sand are the same due to using the same Sh_c . If Sh_c is increased from 2 to 2.5, the rate of capillary rise will be decrease or spending more time to reach the maximum level (Figure 4.3).

Comparison between experimental data and simulated data for the Column III (non-saline sandy loam) and Column IV (saline sandy loam) are shown in Figure 4.2. Simulated capillary rise from analytical solutions show a good agreement

to the experimental capillary rise at a long time close to the maximum capillary rise. However, analytical solutions give faster rate of capillary rise when moving capillary rise is less than maximum rise. With sensitivity analysis by increasing Sh_c from 3.2 to 5, the analytical solutions show that the rate of capillary rise tend to decrease or take a longer time to arrive maximum rise (Figure 4.4).

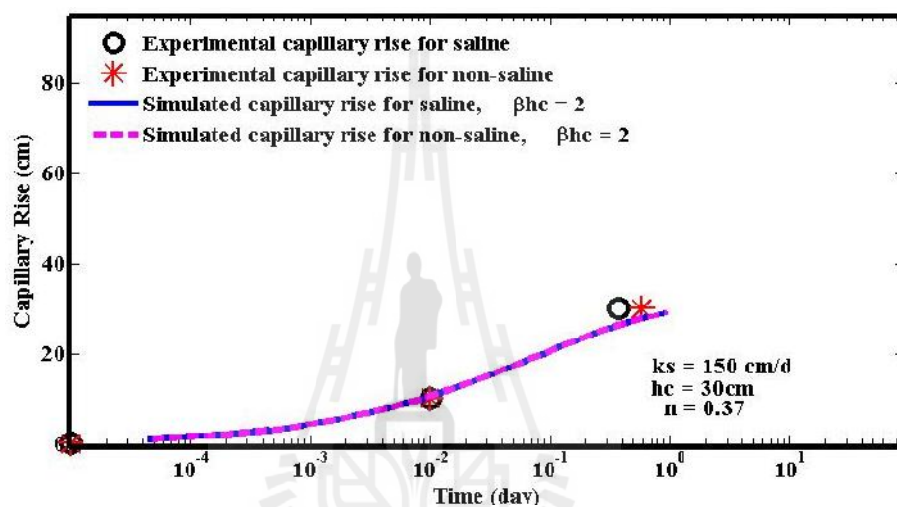


Figure 4.1 The capillary rise vs time for saline and non-saline sand (Column I and II) comparison between E.R of Maskong (2010) and A.S of Lu and Likos (2004) for $Sh_c=2$.

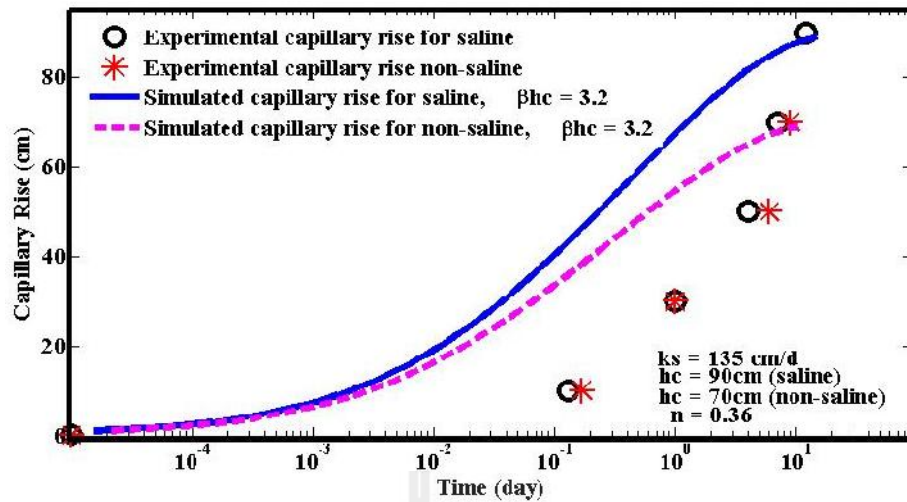


Figure 4.2 The capillary rise vs time for saline and non-saline sandy loam (Column III and IV) comparison between E.R of Maskong (2010) and A.S of Lu and Likos (2004) for $Sh_c=3.2$.

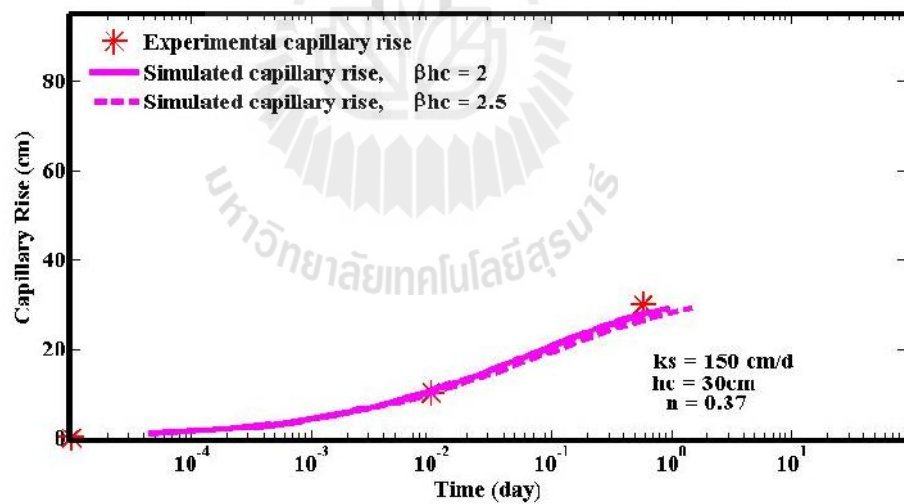


Figure 4.3 The capillary rise vs time for non-saline sand (Column I) comparison between E.R of Maskong (2010) and A.S of Lu and Likos (2004) using $Sh_c=2$ and 2.5.

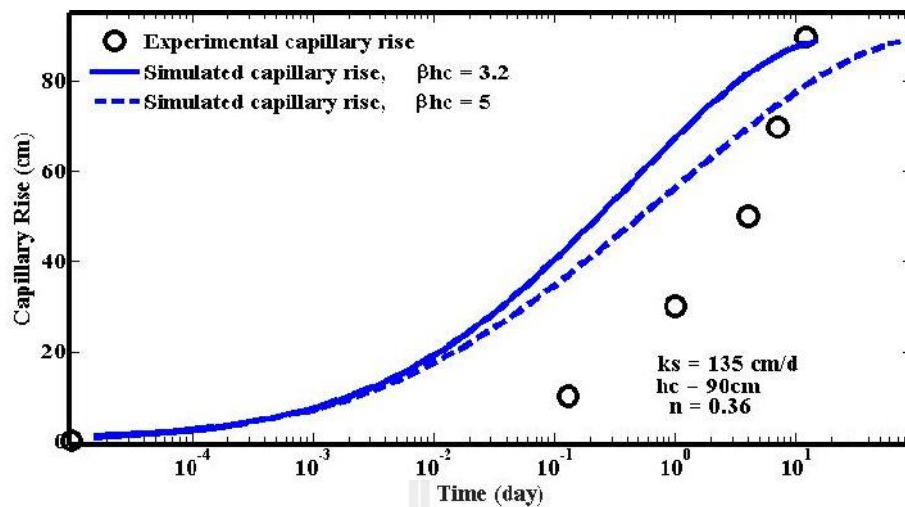


Figure 4.4 The capillary rise vs time for saline sandy loam (Column IV) comparison between E.R of Maskong (2010) and A.S of Lu and Likos (2004) using $Sh_c=3.2$ and 5.

4.3 Richards equation for the capillary flow

4.3.1 Numerical solution

The unsaturated upward movement model, similar to the inverse method (Natthawit, et al., 1995), was developed to obtain the rate of capillary rise and the required SWCC. For comparison, HYDRUS- 1D was also used to solve numerically Richards' equation for one-dimensional capillary flow (Natthawit, et al., 1995).

Simulated numerical results have been generated by using reverse method in form of MATLAB R2010a code (seen in Appendix C). These codes are modified to upward movement from the downward infiltration flow movement given by Jothityangkoon (2011). From Maskong's soil column tests, the moisture content profiles (see in Appendix A) were used to compare with numerical solutions. The five levels of measured capillary rises are 10, 30, 50, 70, 90 cm. By using the reverse

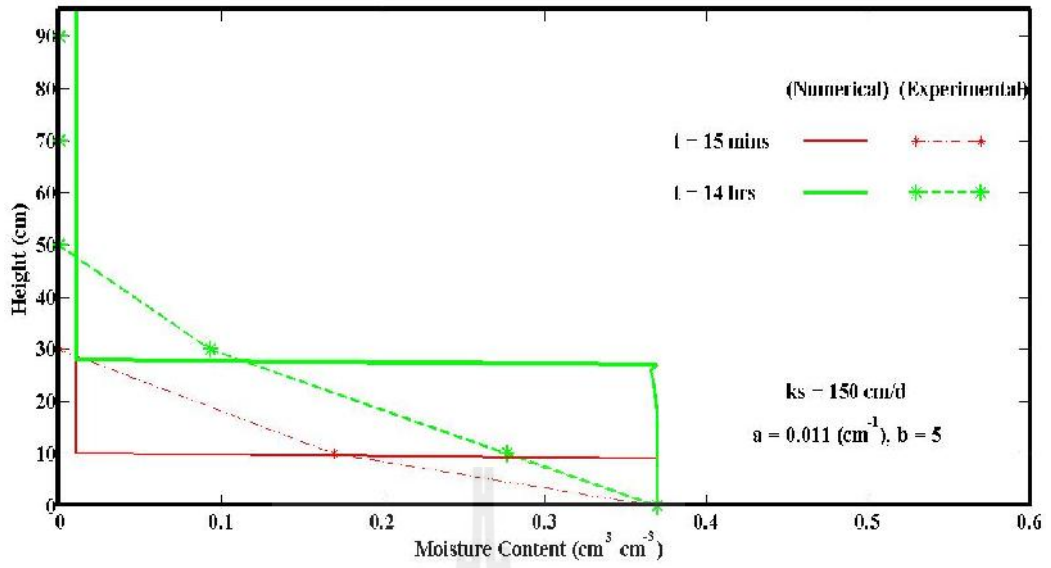
method, simulated rate of capillary rises were estimated given the soil hydraulic properties.

(1) Numerical solution for sand

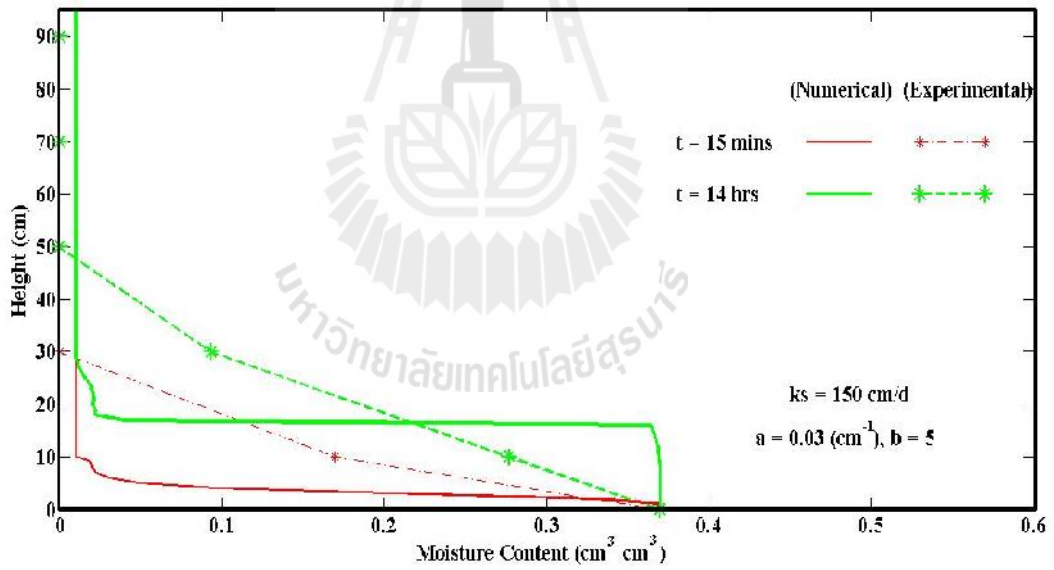
For Column I data, the fitted capillary flow was determined by changing parameters (a and b) in Eq. (3.17) to get the best fit with the data points. Figure 4.5 illustrates the effect of changing parameter a for constant b . Figure 4.6 illustrates the effect of changing parameter b for constant a . In each case, K_s value was the same as K_s using in analytical solution (150 cm/day).

In Figure 4.5, parameter $b = 5$ (fixed) and changing parameter a was from 0.011 to 0.03. When $a = 0.011 \text{ cm}^{-1}$ is used, the simulated result gives good fit to curve gives at shorter time period ($t = 15$ mins), but, gives a little slower rate of capillary rise for the long time period ($t = 14$ hrs), see Figure 4.5(a). The simulated rate of capillary rise tend to decrease when parameters a is increased, see Figure 4.5(b). The calibrated parameters $a = 0.012 \text{ cm}^{-1}$ provides the best fitted curve of N.R to E.R.

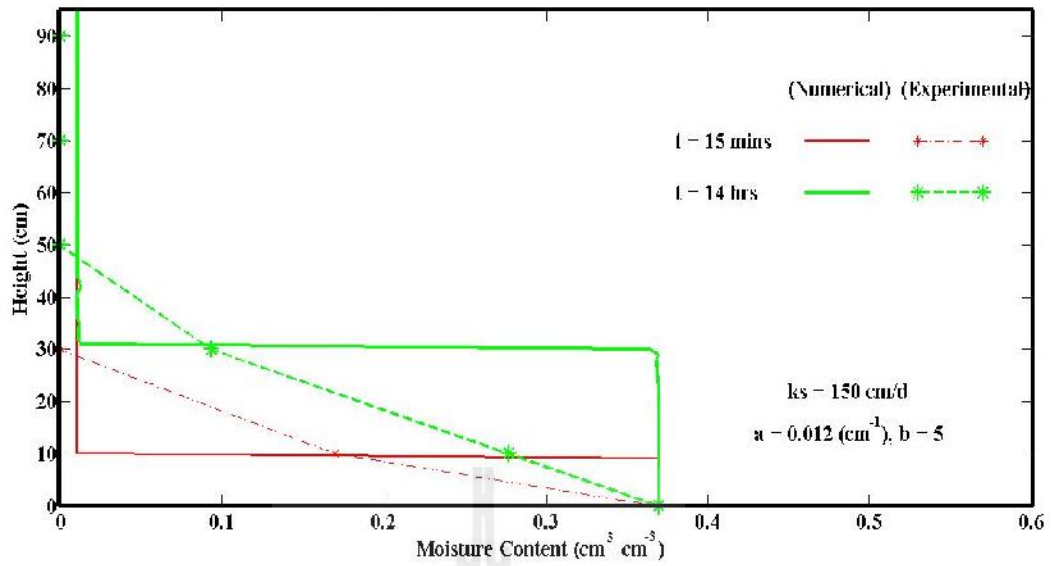
In Figure 4.6, parameter $a = 0.012 \text{ cm}^{-1}$ (fixed) and changing parameter b was from 3 to 6. For short time period ($t = 15$ mins), all N.R show the best fitted curve of N.R to E.R. For long time period ($t = 14$ hrs), the simulated rate of capillary rise tend to decrease when parameter b is decreased, see Figure 4.6(a). And conversely, this rate increased when parameter b is increased, see Figure 4.6(b)). So, the calibrated parameters $a = 0.025 \text{ cm}^{-1}$ and $b = 3$ provide the fitted curve (Figure 4.6(c)).



(a)



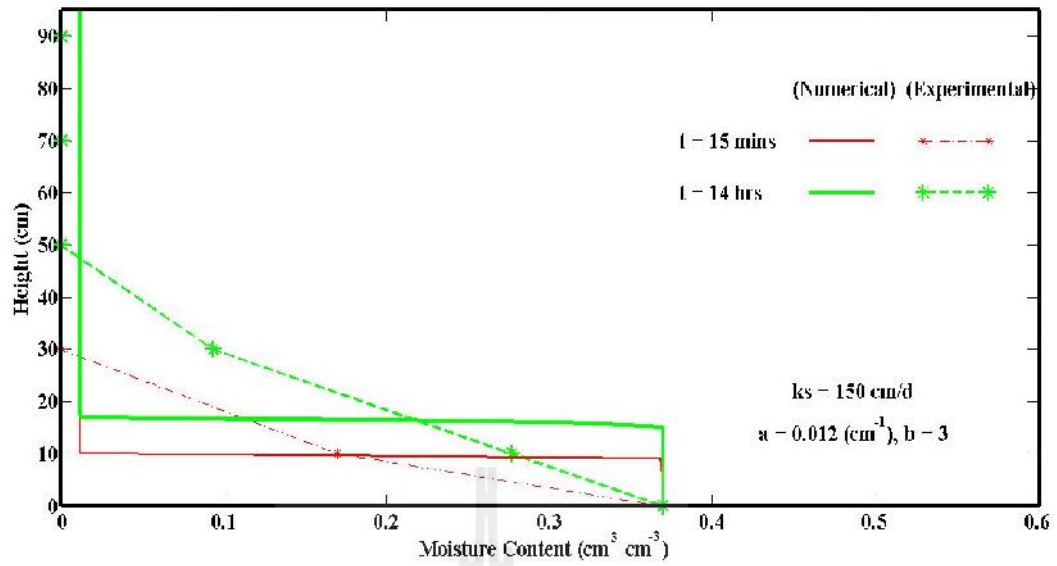
(b)



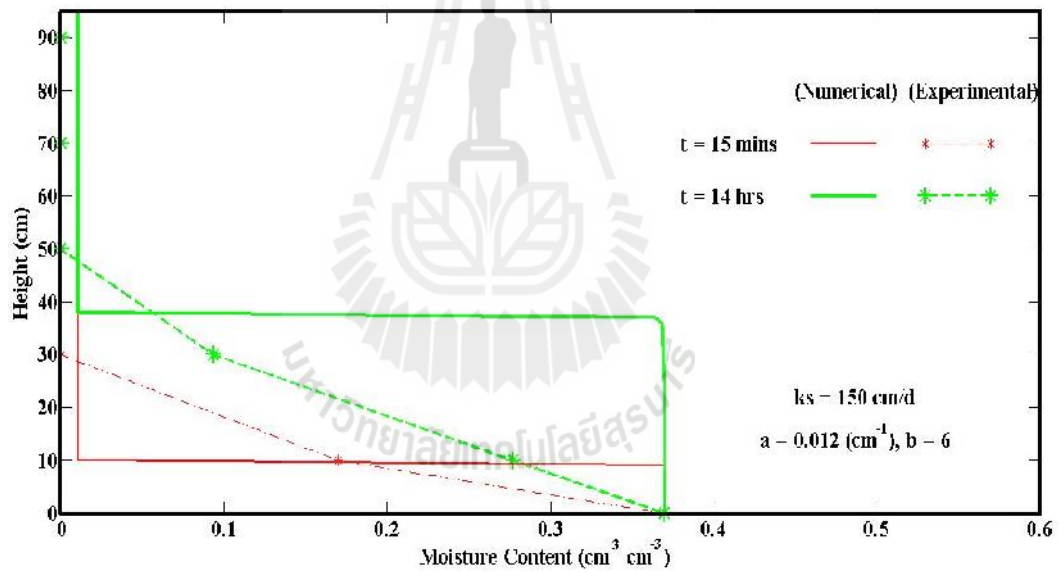
(c)

Figure 4.5 The relationship between capillary height and moisture content for Column I. Comparison of experimental and simulated results using numerical model applied van Genuchten (1980) equation with changing parameter a .

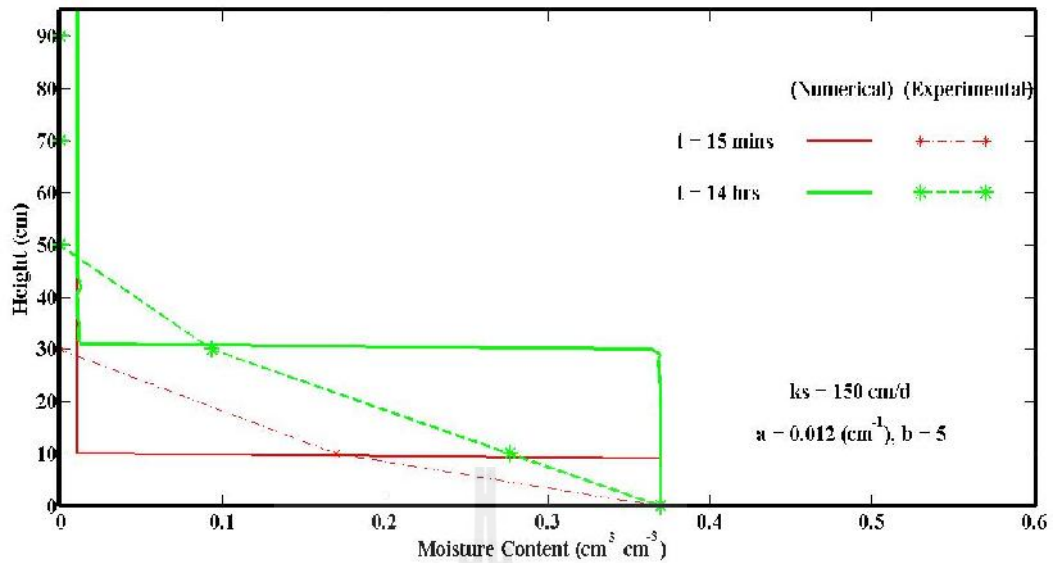
(a) parameter $a = 0.011 \text{ cm}^{-1}$ (b) parameter $a = 0.03 \text{ cm}^{-1}$ (c) parameter $a = 0.012 \text{ cm}^{-1}$



(a)



(b)



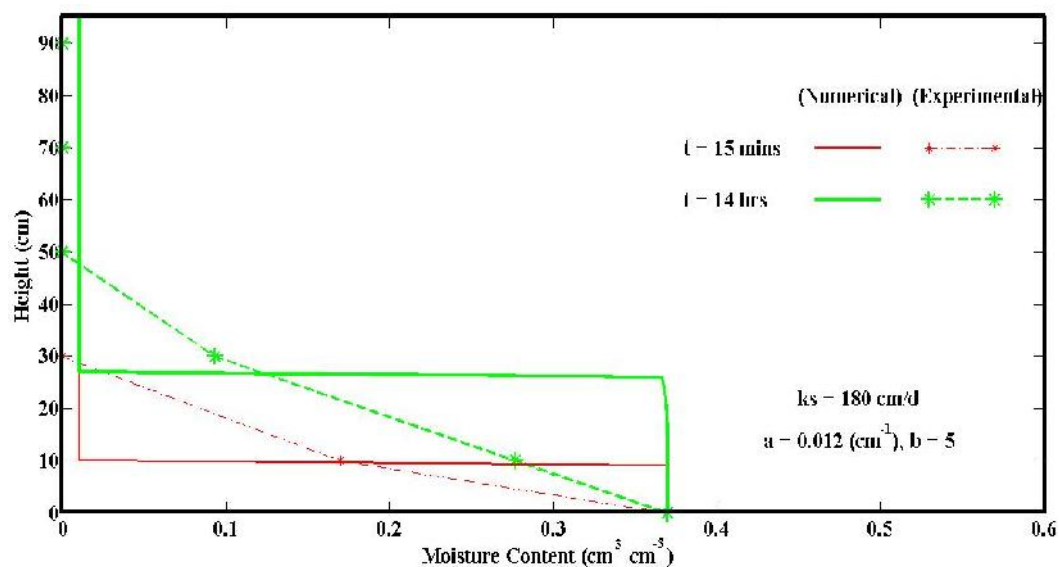
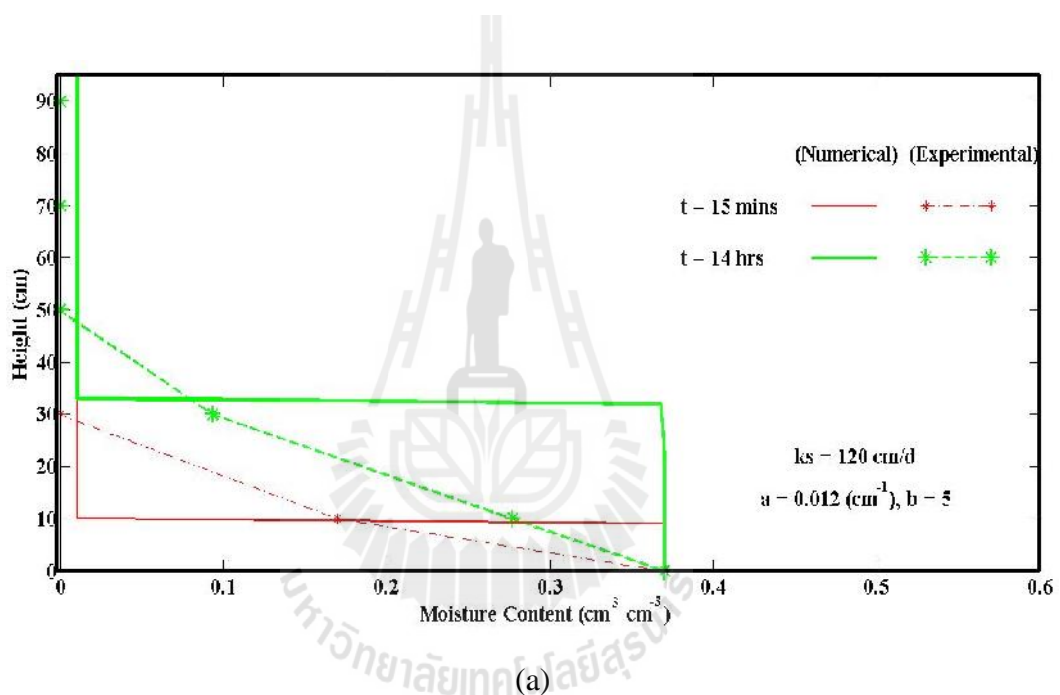
(c)

Figure 4.6 The relationship between capillary height and moisture content for Column I. Comparison of experimental and simulated results using numerical model applied van Genuchten (1980) equation with changing parameter b .

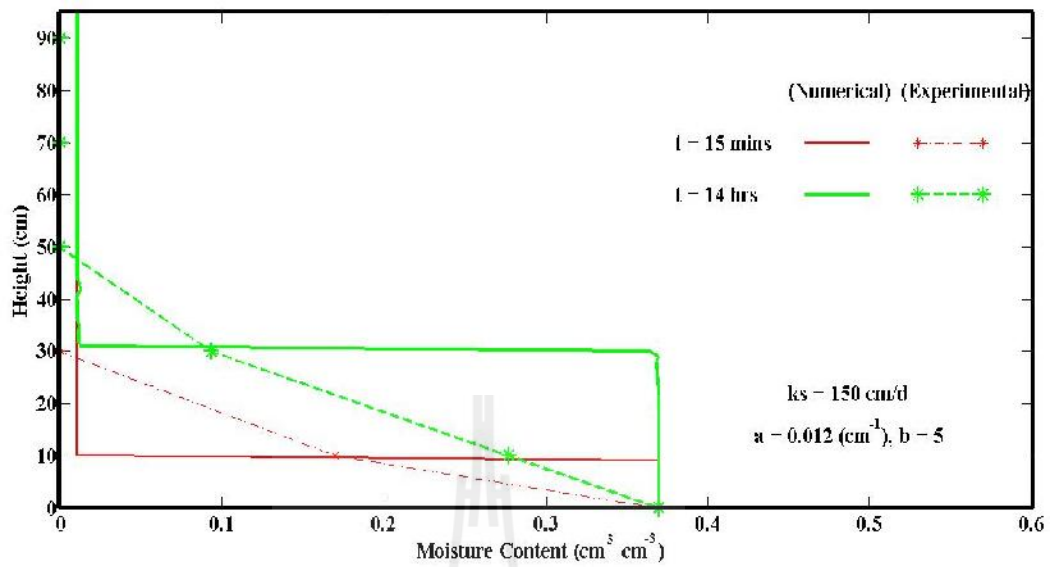
(a) parameter $b = 3$ (b) parameter $b = 6$ (c) parameter $b = 5$

In Figure 4.7, parameter K_s is varied from 120 cm/d to 180 cm/d, using optimal value of a and b from previous steps. For short time period ($t = 15$ mins), all N.R show underestimated curve of capillary height with moisture content. For long time period ($t = 14$ hrs), the simulated rate of capillary rise tend to increase when parameter K_s is decreased, see Figure 4.7(b)). And conversely, this rate increased when parameter K_s is increased, see Figure 4.7(b)). $K_s = 150$ cm/d presents a better agreement between N.R and E.R, see Figure 4.7(c). These optimal calibrated parameters are $a = 0.012$ cm⁻¹, $b = 5$ and $K_s = 150$ cm/d.

According to the above analyzing steps, the fitted capillary flows for the soil Column II, III and IV were performed. K_s were used the same values for saline and non-saline soils. From the result of soil Column II, the simulated capillary rates with parameters ($a = 0.02 \text{ cm}^{-1}$, $b = 5$ and $K_s = 150 \text{ cm/d}$) give the best fit curve of N.R to E.R expect a little faster than E.R at long time period ($t = 9 \text{ hrs}$) (Figure 4.8).



(b)



(c)

Figure 4.7 The relationship between capillary height and moisture content for Column I. Comparison of experimental and simulated results using numerical model applied van Genuchten (1980) equation with changing parameter K_s .

(a) parameter $K_s = 120$ cm/d (b) parameter $K_s = 180$ cm/d (c) parameter $K_s = 150$ cm/d

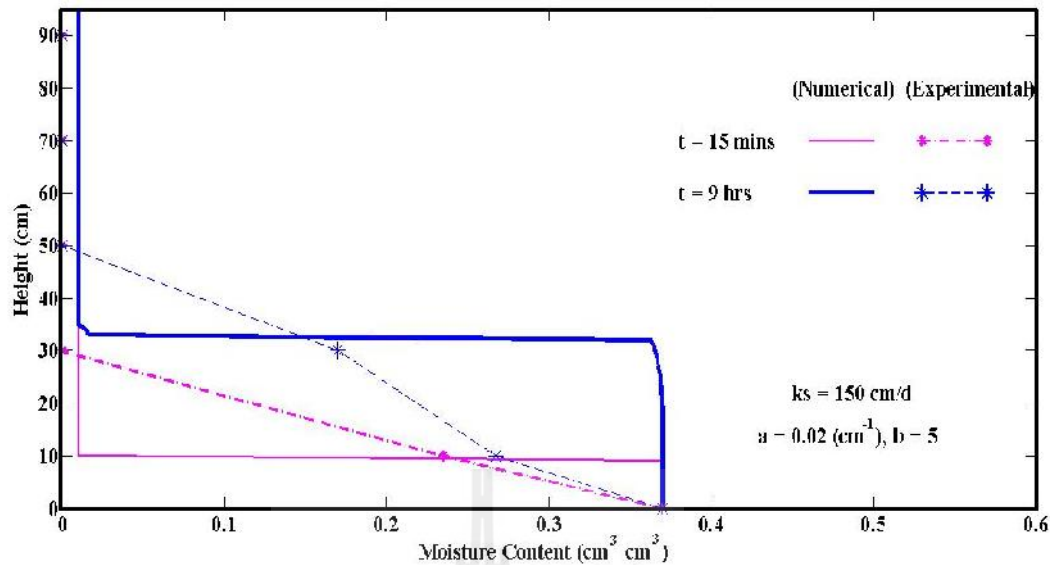


Figure 4.8 The relationship between capillary height and moisture content for Column II. Comparison of experimental and simulated results using numerical model applied van Genuchten (1980) equation with $a = 0.02$ cm⁻¹, $b = 5$ and $K_s = 150$ cm/d.

(2) Numerical solution for sandy loam

Starting from constant bottom moisture content similar to Column I and II numerical results (N.R) for Column III and IV were simulated, and found that rates of capillary rise of N.R are slower than that of experimental results (E.R) for short time period ($t < 24$ hrs). For long time period ($t > 24$ hrs), N.R give faster rate of capillary rise than E.R (Figure 4.9). To capture the reduction and variation of measured moisture content at the low level of soil column, the model was modified to allow the decrease of moisture content with time at the bottom node. This improvement gives a better result, comparing between Figure 4.9 and Figure 4.10. For both short and long time period, N.R (Column III, $a = 0.01$ cm⁻¹, $b = 3.6$ and $K_s = 3$ cm/d) with varying bottom moisture content presents good fit curves of the rate of

capillary rise to E.R better than N.R with constant bottom moisture content. For saline sandy loam in Column IV, see Figure 4.11, N.R (Column IV, $a = 0.01 \text{ cm}^{-1}$, $b = 3.9$ and $K_s = 3 \text{ cm/d}$) from the model including the decrease of moisture content with time also provide good fit curve to E.R, particularly, at $t = 24, 168, 288$ hrs.

Although, the reason of variation of measured soil moisture content along the soil column III and IV can not be identified, relaxing the bottom boundary condition by allowing the decrease of moisture content with time from saturated condition ($t < 24$ hrs) to unsaturated condition ($t > 24$ hrs) gives a good match between moisture content along the column height to E.R, except at the bottom level ($z = 0$).

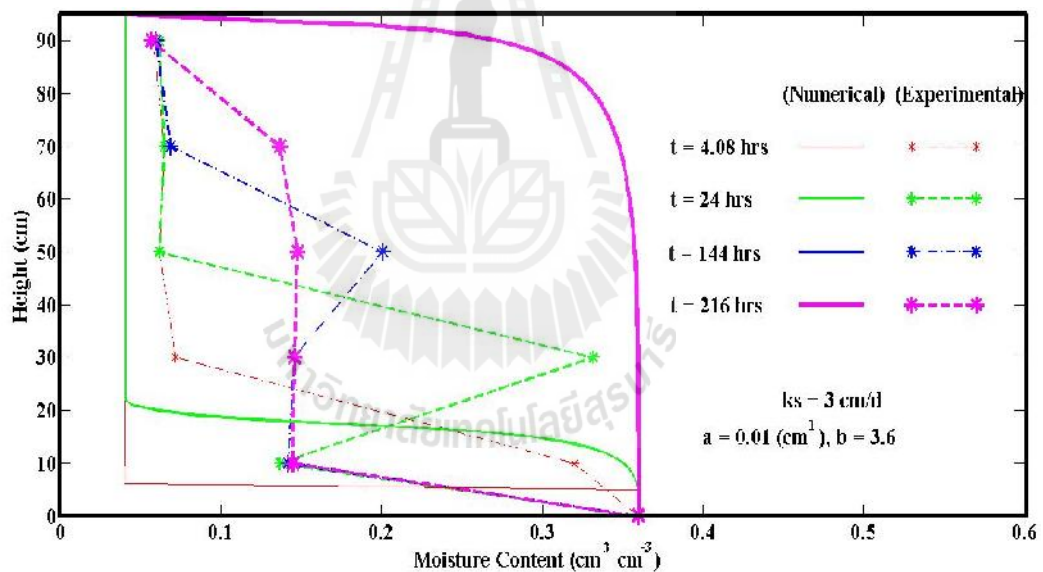


Figure 4.9 The relationship between capillary height and moisture content for Column III. Comparison of experimental and simulated results using numerical model applied van Genuchten (1980) equation with $a = 0.01 \text{ cm}^{-1}$, $b = 3.6$ and $K_s = 3 \text{ cm/d}$ with constant bottom moisture content.

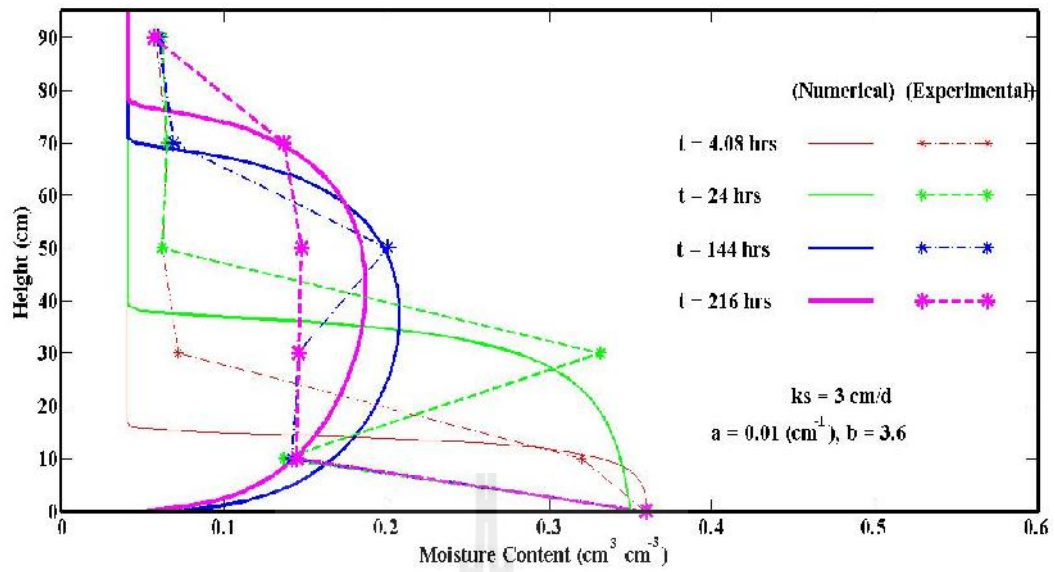


Figure 4.10 The relationship between capillary height and moisture content for Column III. Comparison of experimental and simulated results using numerical model applied van Genuchten (1980) equation with $a = 0.01 \text{ cm}^{-1}$, $b = 3.6$ and $K_s = 3 \text{ cm/d}$ with decreasing bottom moisture content with time.

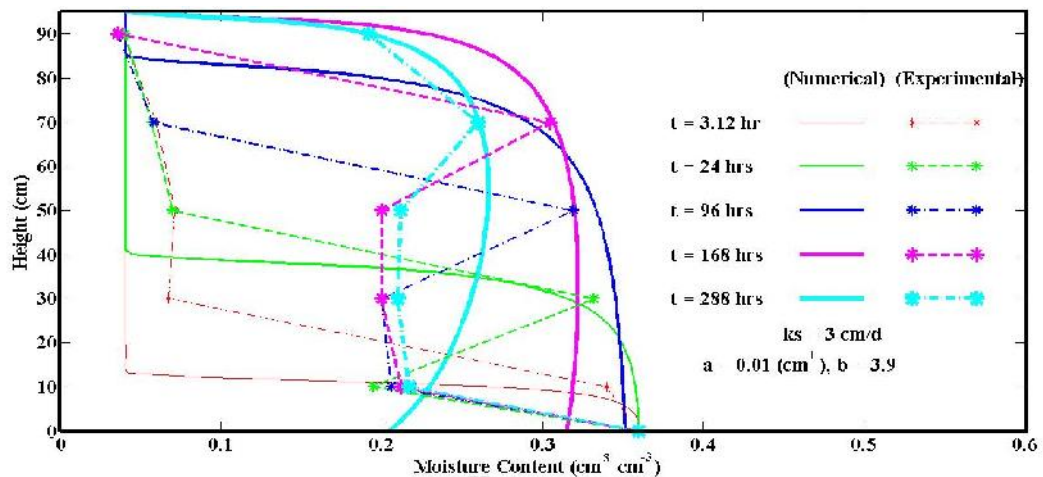


Figure 4.11 The relationship between capillary height and moisture content for Column IV. Comparison of experimental and simulated results using numerical model applied van Genuchten (1980) equation with $a = 0.01 \text{ cm}^{-1}$, $b = 3.9$ and $K_s = 3 \text{ cm/d}$ with decreasing bottom moisture content with time.

4.4 Estimation of maximum capillary heights

The calibrated parameters of the van Genuchten equation for each soil type and condition are shown in Table 4.3. Based on calibrated van Genuchten parameters using inverse method, the resulting SWCC for non saline sand and sandy loam are shown in Figure 4.12. The calculated function for SWCC is described in Appendix C. To estimate maximum capillary height, the analytical solutions are evaluated again using $h_a = 17 \text{ cm}$ (from the SWCC), $K_s = 150 \text{ cm/d}$ for the sand and $h_a = 50 \text{ cm}$ (from the SWCC), $K_s = 3 \text{ cm/d}$ for sandy loam, respectively. For sand, the result is not significantly different between using assuming parameters (h_c and K_s) and the calibrated parameters from UUM model, see Figure 4.1, 4.13. The UUM model can generate a good estimate of the maximum capillary height. In the case of sandy loam,

the result of assuming parameters (Figure 4.1, simulated capillary rise) shows the faster rate of capillary rise compared to that of calibrated parameters (Figure 4.14, simulated capillary rise). Analytical solutions using calibrated soil parameter provides results better than previous analytical solutions using parameters from literatures. Numerical results give a perfect fit to the experimental results (Figure 4.14, 4.15). By using calibrated soil parameters from inversed method, UUM model can estimate simulated maximum capillary rise fit to the experimental capillary rise.

Table 4.3 The calibrated van Genuchten parameters for each soil type and condition

Soil	a (cm ⁻¹)	b	K_s (cmd ⁻¹)
Non-saline sand	0.012	5	150
Saline sand	0.02	5	150
Non-saline sandy loam	0.01	3.6	3
Saline sandy loam	0.01	3.9	3

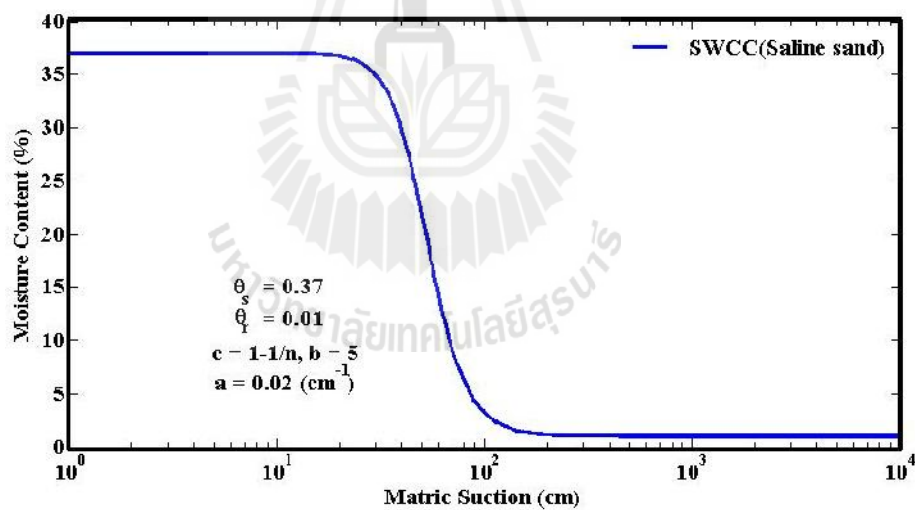
4.5 Calibrated van Genuchten parameters and their physical properties

The calibrated parameter a , based on van Genuchten's equation in Eq. (3.17), represents the inverse of air entry pressure which can be obtained from SWCC curve. Generally, the measured air entry pressure head of sandy loam is higher than that of sand. Therefore, a for sandy loam is lower than a for sand. By using reverse method in this study, calibrated a is found to be 0.01 cm⁻¹ and 0.012 cm⁻¹ for sandy loam and sand, respectively. Although, the values of both calibrated parameters go along with

the definition of a . The difference of them is too small. From literature, a for sandy loam is 0.008 cm^{-1} .

The parameter b , based on van Genuchten's equation in Eq. (3.17), represents the pore size distribution of the soil. More uniform distribution provides higher value of b . The estimated parameters b for sand and sandy loam are 5 and 3.6, respectively. This means the pore size distribution of sand is more uniform than the pore size distribution of sandy loam and this reflect typical properties of sand and sandy loam.

For parameter K_s , calibrated value is 150 cm/d for sand which similar to typical value of K_s from literature. For sandy loam, the calibrated parameter K_s value is 3 cm/d . It is much less than K_s value (135 cm/d) from literature.



(a)

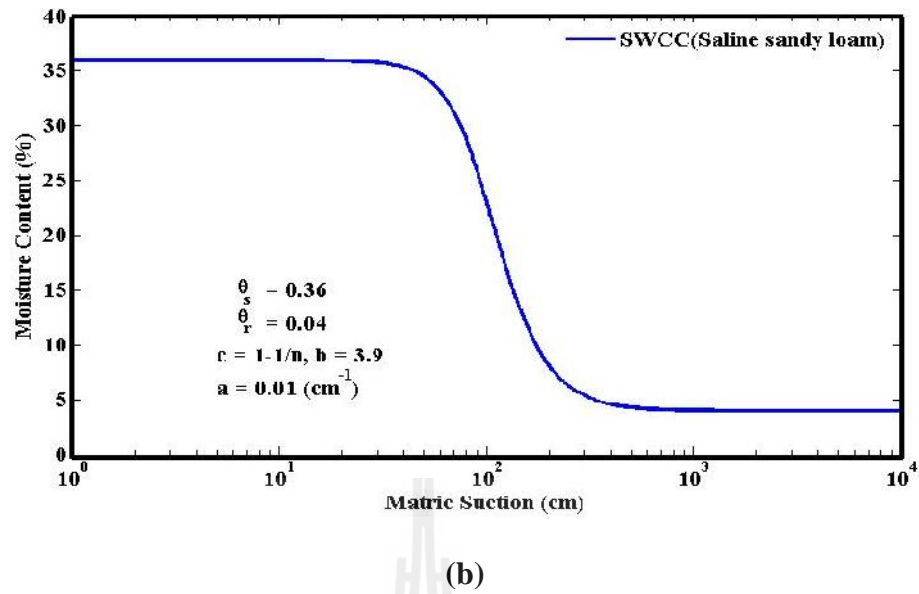


Figure 4.12 The resulting SWCCs of the van Genuchten (1980) equation

for saline soils.

(a) for sand (b) for sandy loam

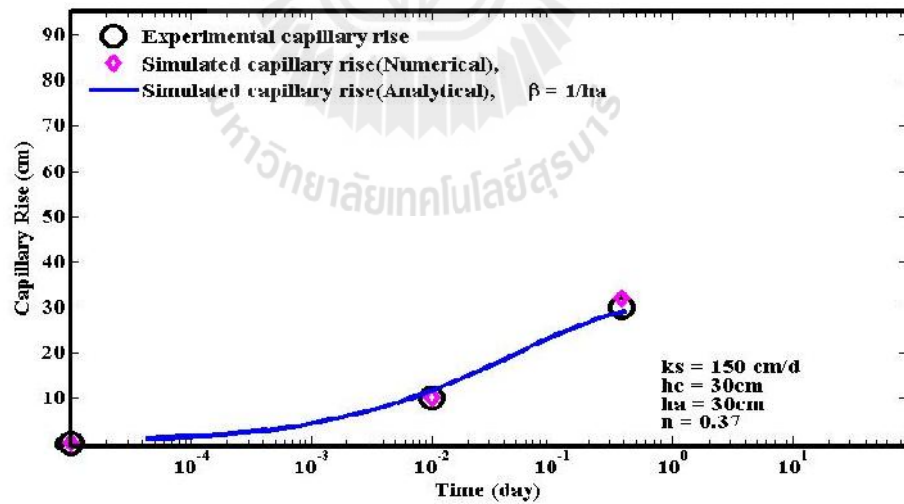


Figure 4.13 The capillary rise vs time for saline sand (Column II) comparison

between E.R of Maskong (2010) and A.S of Lu and Likos (2004)

using $S = 1/ha$.

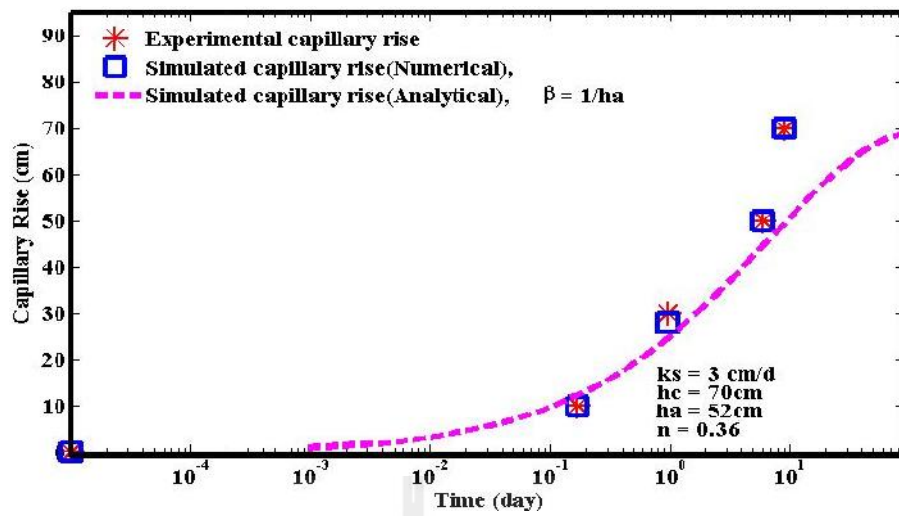


Figure 4.14 The capillary rise vs time for non-saline sandy loam (Column III) comparison between E.R of Maskong (2010) and A.S of Lu and Likos (2004) using $s = 1/h_a$.

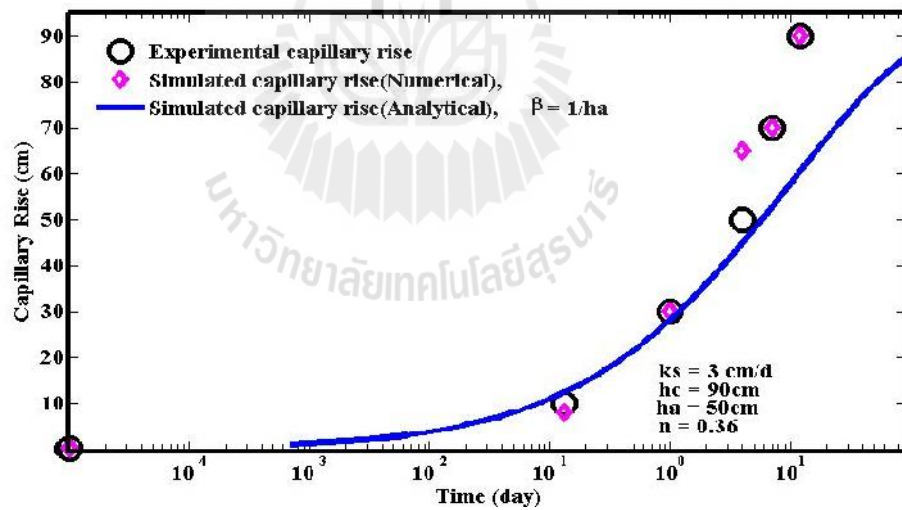


Figure 4.15 The capillary rise vs time for saline sandy loam (Column IV) comparison between E.R of Maskong (2010) and A.S of Lu and Likos (2004) using $s = 1/h_a$.

CHAPTER V

CONCLUSIONS AND RECOMMENDATIONS

5.1 Conclusions

The experimental maximum capillary height with time from Maskong (2010) are analyzed and simulated by using analytical model based on 3 parameters $(1/h_a)$, K_s , and n (Lu and Likos, 2004). These parameters are estimated from the experimental of Maskong (2010) and literatures. The effect of saline water to these parameters is very small for sand. So, analytical solutions give no difference between saline and non-saline on maximum capillary height. For sandy loam, analytical solutions always give fast increase of capillary rise, especially, during initial time period.

For numerical solution, the unsaturated upward movement model is developed based on Richards' equation for one dimensional capillary flow. Using the concept of inversed method, parameters for the model are calibrated respect to experimental results of Maskong (2010). Given the best fitted curves, these parameters are $a = 0.012 \text{ cm}^{-1}$, $b = 5$ and $K_s = 150 \text{ cm/d}$ for sand, and the reverse method with these parameters give a good prediction of the rate of capillary rise in non-saline sand (Column I). To receive the best fitted curves for sandy loam, bottom boundary conditions have to change from constant to varying moisture content with time. The decrease of bottom moisture content with time allow numerical model provide better fitted curve with parameters $a = 0.01 \text{ cm}^{-1}$, $b = 3.6$ and $K_s = 3 \text{ cm/d}$ for Column III and $a = 0.01 \text{ cm}^{-1}$, $b = 3.9$ and $K_s = 3 \text{ cm/d}$ for Column IV.

These parameters can be used to construct SWCC curve in wetting direction. A new set of parameters for analytical model can be estimated from the SWCC curve. Both analytical and numerical model based on calibrated parameters generate a good estimate of maximum capillary height. These models may be used to solve the engineering problems involving time dependent wetting processes resulting from capillary rise, whereas it's suitable for the short durations and capillary rise in shallow groundwater.

5.2 Recommendations

The variation of moisture content with different level of soil column can not be physically explained from this study. The fluctuation of moisture content from one level to another level may cause from non-uniform upward flow in unsaturated condition. The effect of osmotic suction play important role for saline sandy loam. However, this effect is not included in numerical model and left for further study.

REFERENCES

- Arunin,S. (1987). Management of saline and alkaline soils in Thailand, **Paper presented at the Regional Expert Consultation on the Management of Saline/Alkaline Soils**, FAO, Bangkok: FAO Regional Office for Asia and the Pacific.
- Bear, J. (1978). **Hydraulics of groundwater**. New York & London: McGraw-Hill Int Book Co, pp. 569.
- Fredlund, D.G., and Rahardjo, H. (1993). **Soil mechanics for unsaturated soils**. New York: Wiley.
- Gardner, W.R. (1958). Some steady state solutions of the unsaturated moisture flow equation with application to evaporation from a water table. **Soil Science**, 85, No.4, pp. 228-232.
- Gradshteyn, I.S., Ryzhik, I.M., and Jeffrey, A. (1994). **Table of integrals, series, and products**, 5th Ed., Academic, Boca Raton, Fla.
- Ghassemi, F., Jakeman A.J., and Nix, H. (1995). **Salinisation of Land and Water Resources: Human Causes, Extent, Management and Case Studies**. Oxford, CAB International.
- Hillel, D. (1980). **Fundamentals of soil physics**. Academic Press, New York, pp. 413.
- Jitrapinate, N., Sriboonlue, V., Srisuk, K., and Hormdee, D. (2011). Simplified Procedure for Unsaturated Flow Parameters, **American Journal of Applied Sciences**, 8 (6): pp.635-643.

- Jothityangkoon, C. (2012). Modeling of hydrological processes, **Lecture notes**. School of Civil Engineering, Suranaree University of Technology, Nakhonratchasima, Thailand.
- Kumar, S. and Malik, R.S. (1990). Verification of quick capillary rise approach for determining pore geometrical characteristics in soils of varying texture. **Soil Science**, Vol. 150, No. 6, pp. 883-888.
- Konyai, S., Sriboonlue, V., and Trelo-ges, V. (2009). The Effect of Air Entry Values on Hysteresis of Water Retention Curve in Saline Soil, **American Journal of Environmental Sciences**, 5: pp. 341-345.
- Lane, K.S., and Washburn, S.E. (1946). Capillary tests by capillarimeter and by soil filled tubes. **Proc. Highway Research Board**, 26, pp. 460–473.
- Loffler, E., and Kubiniok, J. (1988). Soil salinization in north-east Thailand. **Erdkunde**, 42: pp. 89-100.
- Lu, N., and Likos, W. (2004). **Unsaturated soil mechanics**. New Jersey: Wiley.
- Mualem, Y. (1976). A new model for predicting the hydraulic conductivity of unsaturated porous media. **Water Resources Res**, 12(3): pp. 513–522.
- Malik, R.S., Kumar, S., and Malik, R.K. (1989). Maximal capillary rise flux as a function of height from the water table. **Soil Sci.**, 148(5), pp. 322–326.
- Maskong, H. (2010). Capillary cut for salinity control in sandy loam, **M. Thesis**, School of Civil Engineering, Suranaree University of Technology, Nakhonratchasima, Thailand.
- Murray, E.J., and Sivakumar, V. (2010) **Unsaturated Soils: A fundamental interpretation of soil behavior**. John Wiley & Sons, pp. 1-3.

- Office of geology. (2005). **Geology of study area on geologic factors causing soil salinity in north-east region**. Department of mineral resources.
- Richards, L.A. (1931). Capillary conduction of liquids through porous mediums. **Physics**, 1(5): pp. 318-333.
- Reynolds, W.D., and Topp, G.C. (2008). “Soil water desorption and imbibition: tension and pressure techniques.” **Soil sampling and methods of analysis**, 2nd ed. CRC Press, Boca Raton, FL, pp. 981-998.
- Sinanuwong, S., and Takaya, Y. (1974). Their possible origin as deduced from field evidence, **Southeast Asian Studies**, 12, N0.1.
- Sinanuwong, S., and Takaya, Y. (1974). Their possible origin as deduced from field evidence, **Southeast Asian Studies**, 12, N0.3.
- Smedema, L.K., and Rycroft D.W. (1983). **Land drainage : planning and design of Agricultural Drainage Systems**. Batsford, London, pp. 376.
- Terzaghi, K. (1943). **Theoretical Soil Mechanics**. New York: Wiley.
- Tindall, J.A., Kunkel, J.R., and Anderson, D.E. (1999). **Unsaturated Zone Hydrology for scientists and engineers**. New Jersey: Prentice Hall, Inc.
- van Genuchten, M.T., (1980). A closed-form equation for predicting hydraulic conductivity of unsaturated soils. **Soil Sci**, J 44(5): pp. 892–898.



APPENDIX A

PREVIOUS EXPERIMENTAL DATA

Table A.1 Properties of material in laboratory

Soil properties	Unit	Value
Sand		
○ Diameter of soil	mm	0.25 - 0.45
○ Specific gravity	-	2.67
○ Dry density	g/cm ³	1.68
○ Porosity	-	0.37
○ Initial of salty, EC	dS/m	0
Sandy loam		
○ Clay	%	1
○ Silt	%	37
○ Sand	%	62
○ Specific gravity	-	2.64
○ Dry density	g/cm ³	1.7
○ Porosity	-	0.36
○ Initial of salty, EC	dS/m	0.05
Water		
○ NaCl	%	10
○ Initial of salty, EC	dS/m	0
○ Density of saline water	g/cm ³	1.10
○ Density of non-saline water	g/cm ³	1.00

Table A.2 The relationship between soil moisture content vs time for each soil levels

(z) of soil Column I.

Time	Column I				
(min)	Z=-85 cm	Z=-65 cm	Z=-45 cm	Z=-25 cm	Z=-5 cm
0	0	0	0	0	0
5	0	0	0	0	0
10	3.435	0	0	0	0
15	17.088	0	0	0	0
20	28.26	0	0	0	0
25	28.405	0	0	0	0
30	28.308	0	0	0	0
60	28.211	0	0	0	0
120	28.26	1.772	0	0	0
180	28.211	3.019	0	0	0
240	28.211	4.821	0	0	0
300	28.017	6.068	0	0	0
360	28.066	6.346	0	0	0
420	27.968	7.177	0	0	0
480	28.114	7.732	0	0	0
540	28.017	8.286	0	0	0
600	27.871	8.563	0	0	0
660	27.871	8.979	0	0	0
720	27.773	8.979	0	0	0
780	27.773	8.979	0	0	0

Table A.2 The relationship between soil moisture content vs time for each soil levels

(z) of soil Column I. (Continued)

Time	Column I				
(min)	Z=-85 cm	Z=-65 cm	Z=-45 cm	Z=-25 cm	Z=-5 cm
840	27.773	9.533	0	0	0
900	27.724	9.533	0	0	0
960	27.773	10.088	0	0	0
1020	27.773	10.088	0	0	0
1080	27.822	10.088	0	0	0
1140	27.773	10.504	0	0	0
1200	27.822	10.642	0	0	0
1260	27.822	10.504	0	0	0
1320	27.871	10.642	0	0	0
1380	27.773	10.504	0	0	0
1440	27.773	10.504	0	0	0

Table A.3 The relationship between soil moisture content vs time for each soil levels

(z) of soil Column II.

Time	Column II				
(min)	Z=-85 cm	Z=-65 cm	Z=-45 cm	Z=-25 cm	Z=-5 cm
0	0	0	0	0	0
5	0	0	0	0	0
10	0.03	0	0	0	0
15	23.51	0	0	0	0
20	25.63	0	0	0	0
25	25.87	0	0	0	0
30	26.06	0	0	0	0
60	26.54	0	0	0	0
120	27.35	4.06	0	0	0
180	27.73	9.31	0	0	0
240	27.1	12.82	0	0	0
300	26.99	14.72	0	0	0
360	26.9	15.71	0	0	0
420	27.04	16.32	0	0	0
480	26.82	16.76	0	0	0
540	26.75	17	0	0	0
600	26.64	17.13	0	0	0
660	26.59	17.18	0	0	0
720	26.75	17.19	0	0	0
780	26.7	17.18	0	0	0

Table A.3 The relationship between soil moisture content vs time for each soil levels

(z) of soil Column II. (Continued)

Time	Column II				
(min)	Z=-85 cm	Z=-65 cm	Z=-45 cm	Z=-25 cm	Z=-5 cm
840	26.54	17.23	0	0	0
900	26.51	17.21	0	0	0
960	26.49	17.23	0	0	0
1020	26.44	17.25	0	0	0
1080	26.51	17.21	0	0	0
1140	26.49	17.19	0	0	0
1200	26.47	17.21	0	0	0
1260	26.47	17.21	0	0	0
1320	26.37	17.21	0	0	0
1380	26.51	17.21	0	0	0
1440	26.51	17.21	0	0	0

Table A.4 The relationship between soil moisture content vs time for each soil levels

(z) of soil Column III.

Time	Column III				
(day)	Z=-85 cm	Z=-65 cm	Z=-45 cm	Z=-25 cm	Z=-5 cm
0	6.7	7.3	6.3	6.6	5.9
0.04	6.7	7.2	6.2	6.5	5.8
0.08	6.7	7.2	6.2	6.5	5.8
0.13	21.5	7.2	6.2	6.5	5.8
0.17	32	7.2	6.2	6.5	5.8
0.21	31.8	7.1	6.2	6.5	5.8
0.25	28.6	7.1	6.2	6.5	5.7
0.29	26.3	7.1	6.2	6.5	5.7
0.33	25.2	7.1	6.2	6.4	5.7
0.38	24.8	7.1	6.1	6.4	5.7
0.42	23.3	7.1	6.1	6.4	5.7
0.46	22.8	7	6.1	6.4	6.1
0.5	20.2	7	6.1	6.4	6.1
0.54	19.7	7	6.1	6.4	6.1
0.58	17.8	7.1	6.1	6.4	6.1
0.63	16.4	7.1	6.1	6.4	6.1
0.67	15.4	7.1	6.2	6.4	6.2
0.71	14.6	7.3	6.2	6.4	6.2
0.75	13.9	8.7	6.2	6.4	6.2
0.79	13.6	9	6.2	6.5	6.2

Table A.4 The relationship between soil moisture content vs time for each soil levels

(z) of soil Column III. (Continued)

Time (day)	Column III				
	Z=-85 cm	Z=-65 cm	Z=-45 cm	Z=-25 cm	Z=-5 cm
0.83	13.5	10.1	6.2	6.5	6.2
0.88	13.5	13.7	6.2	6.5	6.2
0.92	13.5	20.2	6.2	6.5	6.2
0.96	13.7	24.4	6.3	6.5	6.2
1	13.7	33.2	6.2	6.5	6.2
2	13.9	22.8	6.3	6.5	6.2
3	13.9	16.8	32.7	6.5	6.3
4	14	14.9	33.6	6.6	6.3
5	14.1	14.8	31.9	6.8	6.1
6	14.2	14.6	20.1	6.9	6
7	14.3	14.8	16.8	7.1	5.9
8	14.4	14.7	14.9	10.1	5.8
9	14.5	14.6	14.8	13.7	5.7
10	14.6	14.7	14.6	20.2	5.7
11	14.7	14.8	14.8	24.4	5.8
12	14.7	14.4	14.7	33.2	5.8
13	14.8	15.1	14.6	33.7	5.6
14	14.9	14.6	14.7	33.5	5.8
15	15	14.9	14.8	33.7	5.7
16	15.1	14.6	14.4	33.3	5.6

Table A.4 The relationship between soil moisture content vs time for each soil levels

(z) of soil Column III. (Continued)

Time (day)	Column III				
	Z=-85 cm	Z=-65 cm	Z=-45 cm	Z=-25 cm	Z=-5 cm
17	15.2	14.5	15.1	33.6	5.6
18	15.3	14.5	14.6	33.5	5.7
19	15.4	14.5	14.9	33.4	5.7
20	15.5	14.7	14.6	33.3	5.6
21	15.2	14.7	14.5	33.4	5.4
22	15.2	14.9	14.5	33.3	5.5
23	15.8	14.9	14.5	33.3	5.5
24	14.9	14	14.7	33.3	5.4
25	14.9	14.1	14.7	33.3	5.5
26	14	14.2	14.9	33.3	5.4
27	15.1	14.3	14.9	33.3	5.5
28	15.2	14.4	14	33.2	5.4
29	15.3	14.5	14.1	33.6	5.3
30	15.4	14.6	14.2	33.5	5.3

Table A.5 The relationship between soil moisture content vs time for each soil levels

(z) of soil Column IV.

Time	Column IV				
(day)	Z=-85 cm	Z=-65 cm	Z=-45 cm	Z=-25 cm	Z=-5 cm
0.00	7.2	6.7	7.2	6	3.8
0.02	7.2	6.7	7.2	6	3.8
0.04	7.2	6.8	7.2	6	3.8
0.08	9.6	6.7	7.1	6	3.8
0.13	34	6.7	7.1	6	3.8
0.17	24.5	6.7	7.1	5.9	3.8
0.21	22	6.6	7.1	5.9	3.8
0.25	20.3	6.6	7.1	5.9	3.8
0.29	19.6	6.7	7.1	5.9	3.8
0.33	19.2	6.7	7.1	6	3.8
0.38	19.1	6.7	7.1	6	3.8
0.42	19.1	6.7	7.1	5.9	3.8
0.46	19.1	6.7	7.1	5.9	3.8
0.50	19.1	6.6	7.1	5.9	3.8
0.54	19.1	6.7	7	5.9	3.8
0.58	19.1	6.7	7	5.9	3.8
0.63	19.1	6.7	7	5.9	3.8
0.67	19.2	6.9	7	5.9	3.8
0.71	19.3	7.4	7	5.9	3.8
0.75	19.3	8.3	7	5.9	3.8

Table A.5 The relationship between soil moisture content vs time for each soil levels

(z) of soil Column IV. (Continued)

Time	Column IV				
(day)	Z=-85 cm	Z=-65 cm	Z=-45 cm	Z=-25 cm	Z=-5 cm
0.79	19.3	10.2	7	5.9	3.8
0.83	19.4	16.3	7	5.9	3.8
0.88	19.4	21.8	7	5.9	3.8
0.92	19.4	24	7.1	5.9	3.8
0.96	19.5	25.2	7.1	5.9	3.8
1	19.5	33.2	7	5.7	4
2	19.9	18.6	30.7	5.8	4
30	22.1	21.7	21.8	22.2	35.9
31	22	21.5	21.4	22.2	41
32	22.1	21.6	21.6	22.2	39
33	22.2	21.7	21.8	22.4	41
34	22.3	21.5	21.4	22.2	39
35	22.3	21.5	21.4	22.5	41
36	22.5	21.1	21.8	22.1	41
37	22.5	21.2	21.8	22.3	42
38	22.5	21.3	22	22.2	41
39	22.5	21.2	21.9	22.2	41
40	22.5	21.1	21.8	22.4	41
41	22.5	21.1	21.9	22.2	41
42	22.4	21.1	21.8	22.5	41

Table A.5 The relationship between soil moisture content vs time for each soil levels

(z) of soil Column IV. (Continued)

Time (day)	Column IV				
	Z=-85 cm	Z=-65 cm	Z=-45 cm	Z=-25 cm	Z=-5 cm
43	22.4	21.1	21.8	22.1	41
44	22.2	21	21.6	22.3	41
45	22.3	21	21.7	22.1	41
46	22.3	21	21.7	22.3	41
47	22.5	21.1	21.8	22.2	41
48	22.5	21	21.8	22.5	41
49	22.6	21.1	21.9	22.1	41
50	22.5	21	21.8	22.3	41
51	22.4	20.9	21.7	22.2	41
52	22.5	21	21.9	22.2	41
53	22.5	21	21.9	22.2	41
54	22.6	21	22	22.2	41
55	22.6	21	22	22.2	41
56	22.6	21	22	22.2	41
57	22.5	21	22	22.4	42
58	22.4	21	22	22.3	42
59	22.4	21	21.9	22.5	41
60	22.4	20.9	21.9	22.1	41



APPENDIX B

MATLAB CODES FOR ANALYTICAL SOLUTION

BASED ON TERZAGHI'S EQUATION

B.1 The analytical solution for the rate of capillary rise for non-saline sand and saline

sand (assuming h_c value) (Data for Figure 4.1)

```

% Lu and Likkos (2004) Analytical Solution for sand
% Opening summ1.mat file for serise result
% The rate of capillary rise of non saline sand and saline sand
% Assuming beta =2/hc;

hc=30;           % Max CR(cm)
length=95;      % soil column height (cm)
dx=1;           % Space step (cm)
n=round(hc/dx)+1; % Computing Nodes
N=0.37;         % Porosity of sand
ks=150;         % Saturated hydraulic conductivity (cm/d)
                % (1-5 m/d sand)(Smedema and Rycroft, 1983)
z(1)=0;         % Initial condition of z
t(1)=0;         % Initial condition of t
F1=(N/ks);      % cm/d
beta=2/hc;      % hc/ha= between 2 to 5 ( Lane and Washburn,1946)
                % (Malik et al., 1989), and (Kumar and Malik, 1990)
                % Lu and Likos (2004),
m=11;           % s=0 to 10, m=11
O=summ1(hc);    % summation

for i=1:n-1
    G(i)=hc-z(i);
    P(i)=hc./G(i);
    R(i)=log(P(i));
    RR=R(i);
    Z=z(i);
    for j=1:11
        A=(j-1);
        B=j;
        f(j)=factorial(A);
        C(j)=(beta^A)./f(j);
        S(j)=hc^(j);
        SS=S';
        T=SS.*RR;
        t1=T';
        T1(j)=t1(j)-O(i,j);
        T2=T1';
        TT(j)=C(j)*T2(j);
    end
    TTT(i)=sum(TT);
    W(i)=F1*TTT(i);

```

```

    if z<hc
        z(i+1)=z(i)+1;
    end
end
z=0:1:n-2;

% Experimental data (Maskong, 2010)
x=[0.00001 0.01 0.583];
y=[0.00001 10 30];

% Plotting for Experimental capillary rise
k=plot(x,y,'ko','linewidth',2.0,'MarkerSize',15);hold on

% Plotting for Simulated capillary rise (beta=2/hc)
k=plot(W,z,'m','linewidth',3.0);hold on
legend('Experimental capillary rise for non saline','Simulated capillary rise for non
saline,      hc = 2','location','NorthWest');
set(gca,'Xscale','log','fontname','Times New Roman','fontsize',16);
set(gca,'Yscale','linear','fontname','Times New Roman','fontsize',16);
xlabel('Time (day)','fontname','Times New Roman','fontsize',18)
ylabel('Capillary Rise (cm)','fontname','Times New Roman','fontsize',18)
text(0.8,17,'ks = 150 cm/d','fontname','Times New Roman','fontsize',18);
text(0.8,13,'hc = 30cm','fontname','Times New Roman','fontsize',18);
text(0.8,9,'n = 0.37','fontname','Times New Roman','fontsize',18);
axis([0.00001 90 0 95]);

% The rate of capillary rise of saline sand
% Assuming beta =2/hc;

hc=30;           % Max CR(cm)
length=95;      % soil column height (cm)
dx=1;           % Space step (cm)
n=round(hc/dx)+1; % Computing Nodes
N=0.37;         % Porosity of sand
ks=150;         % Saturated hydraulic conductivity (cm/d)
                % (1-5 m/d sand)(Smedema and Rycroft, 1983)
z(1)=0;        % Initial condition of z
t(1)=0;        % Initial condition of t
F1=(N/ks);     % cm/d
beta=2/hc;     % hc/ha= between 2 to 5 ( Lane and Washburn,1946)
                % (Malik et al., 1989), and (Kumar and Malik, 1990)
                % Lu and Likos (2004),
m=11;          % s=0 to 10, m=11
O=summ1(hc);   % summation

```

```

for i=1:n-1
    G(i)=hc-z(i);
    P(i)=hc./G(i);
    R(i)=log(P(i));
    RR=R(i);
    Z=z(i);
    for j=1:11
        A=(j-1);
        B=j;
        f(j)=factorial(A);
        C(j)=(beta^A)./f(j);
        S(j)=hc^(j);
        SS=S';
        T=SS.*RR;
        t1=T';
        T1(j)=t1(j)-O(i,j);
        T2=T1';
        TT(j)=C(j)*T2(j);
    end
    TTT(i)=sum(TT);
    W(i)=F1*TTT(i);
    if z<hc
        z(i+1)=z(i)+1;
    end
end

z=0:1:n-2;
% Experimental data (Maskong, 2010)
x=[0.00001 0.01 0.375];
y=[0.00001 10 30];

% Plotting for Experimental capillary rise
k=plot(x,y,'r*','linewidth',2.0,'MarkerSize',15);hold on

% Plotting for Simulated capillary rise (beta=2/hc)
k=plot(W,z,'m','linewidth',3.0);hold on
legend('Experimental capillary rise for saline ','Simulated capillary rise for saline,
hc = 2','location','NorthWest');
set(gca,'Xscale','log','fontname','Times New Roman','fontsize',16);
set(gca,'Yscale','linear','fontname','Times New Roman','fontsize',16);
xlabel('Time (day)','fontname','Times New Roman','fontsize',18)
ylabel('Capillary Rise (cm)','fontname','Times New Roman','fontsize',18)
text(0.8,17,'ks = 150 cm/d','fontname','Times New Roman','fontsize',18);
text(0.8,13,'hc = 30cm','fontname','Times New Roman','fontsize',18);
text(0.8,9,'n = 0.37','fontname','Times New Roman','fontsize',18);
axis([0.00001 90 0 95]);

```

B.2 The analytical solution for the rate of capillary rise for saline sand (Data for Figure 4.13)

```

% Lu and Likkos (2004) Analytical Solution for sand
% Opening summ1.mat file for serise result
% The rate of capillary rise of saline sand

hc=30;           % Max CR(cm)
ha=30;           % Air entry head(cm)
length=95;      % soil column height (cm)
dx=1;           % Space step (cm)
n=round(hc/dx)+1; % Computing Nodes
N=0.37;         % Porosity of sand
ks=150;         % (From Table 4.3)
                % (1-5 m/d sand)(Smedema and Rycroft, 1983)
z(1)=0;         % Initial condition of z
t(1)=0;         % Initial condition of t
F1=(N/ks);      % cm/d
beta=1/ha;      % (From Figure 4.11(a))
m=11;           % s=0 to 10, m=11
O=summ1(hc);    % summation

for i=1:n-1
    G(i)=hc-z(i);
    P(i)=hc./G(i);
    R(i)=log(P(i));
    RR=R(i);
    Z=z(i);
    for j=1:11
        A=(j-1);
        B=j;
        f(j)=factorial(A);
        C(j)=(beta^A)./f(j);
        S(j)=hc^j;
        SS=S';
        T=SS.*RR;
        t1=T';
        T1(j)=t1(j)-O(i,j);
        T2=T1';
        TT(j)=C(j)*T2(j);
    end
    TTT(i)=sum(TT);
    W(i)=F1*TTT(i);
    if z<hc
        z(i+1)=z(i)+1;
    end
end

```

```

    end
end

% Experimental data (Maskong, 2010)
z=0:1:n-2;
x=[0.00001 0.01 0.375];
y=[0.00001 10 30];
xx=[0.00001 0.01 0.375];
yy=[0.00001 10 32];

% Plotting for Experimental capillary rise

k=plot(x,y,'ko','linewidth',2.0,'MarkerSize',12);hold on

% Plotting for Simulated capillary rise (Numerical)

k=plot(xx,yy,'m*','linewidth',3.0,'MarkerSize',15);hold on

% Plotting for Simulated capillary rise (beta=1/ha)

k=plot(W,z,'b','linewidth',3.0);hold on

legend('Experimental capillary rise','Simulated capillary rise(Numerical)', 'Simulated
capillary rise(Analytical)', 'beta=1/ha','location','NorthWest');

set(gca,'Xscale','log','fontname','Times New Roman','fontsize',16);
set(gca,'Yscale','linear','fontname','Times New Roman','fontsize',16);
xlabel('Time (day)','fontname','Times New Roman','fontsize',18)
ylabel('Capillary Rise (cm)','fontname','Times New Roman','fontsize',18)
text(0.8,18,'ks = 150 cm/d','fontname','Times New Roman','fontsize',18);
text(0.8,15,'hc = 30cm','fontname','Times New Roman','fontsize',18);
text(0.8,12,'hc = 30cm','fontname','Times New Roman','fontsize',18);
text(0.8,9,'n = 0.37','fontname','Times New Roman','fontsize',18);
axis([0.00001 90 0 95]);

% Function file (For saline and nonsaline sand)
% summ1.mat file for serise result

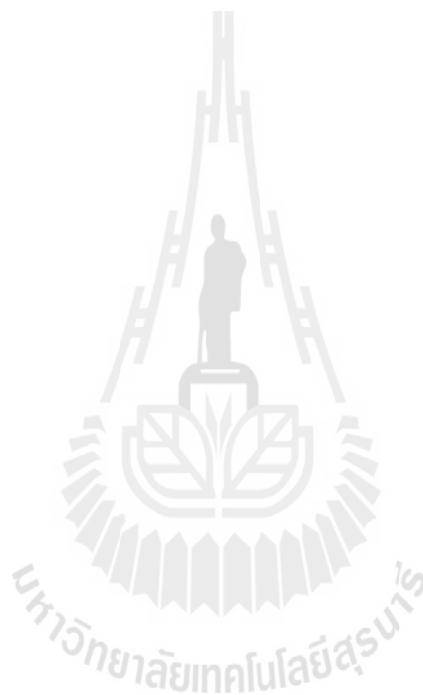
function O=summ1(hc);
Z=0;
[K]=elev(Z,hc);
O(1,:)=K;
Z=1;
[K]=elev(Z,hc);

```

```
O(2,:)=K;
Z=2;
[K]=elev(Z,hc);
O(3,:)=K;
Z=3;
[K]=elev(Z,hc);
O(4,:)=K;
Z=4;
[K]=elev(Z,hc);
O(5,:)=K;
Z=5;
[K]=elev(Z,hc);
O(6,:)=K;
Z=6;
[K]=elev(Z,hc);
O(7,:)=K;
Z=7;
[K]=elev(Z,hc);
O(8,:)=K;
Z=8;
[K]=elev(Z,hc);
O(9,:)=K;
Z=9;
[K]=elev(Z,hc);
O(10,:)=K;
Z=10;
[K]=elev(Z,hc);
O(11,:)=K;
Z=11;
[K]=elev(Z,hc);
O(12,:)=K;
Z=12;
[K]=elev(Z,hc);
O(13,:)=K;
Z=13;
[K]=elev(Z,hc);
O(14,:)=K;
Z=14;
[K]=elev(Z,hc);
O(15,:)=K;
Z=15;
[K]=elev(Z,hc);
O(16,:)=K;
Z=16;
[K]=elev(Z,hc);
O(17,:)=K;
```




```
Z=17;  
[K]=elev(Z,hc);  
O(18,:)=K;  
Z=18;  
[K]=elev(Z,hc);  
O(19,:)=K;  
Z=19;  
[K]=elev(Z,hc);  
O(20,:)=K;  
Z=20;  
[K]=elev(Z,hc);  
O(21,:)=K;  
Z=21;  
[K]=elev(Z,hc);  
O(22,:)=K;  
Z=22;  
[K]=elev(Z,hc);  
O(23,:)=K;  
Z=23;  
[K]=elev(Z,hc);  
O(24,:)=K;  
Z=24;  
[K]=elev(Z,hc);  
O(25,:)=K;  
Z=25;  
[K]=elev(Z,hc);  
O(26,:)=K;  
Z=26;  
[K]=elev(Z,hc);  
O(27,:)=K;  
Z=27;  
[K]=elev(Z,hc);  
O(28,:)=K;  
Z=28;  
[K]=elev(Z,hc);  
O(29,:)=K;  
Z=29;  
[K]=elev(Z,hc);  
O(30,:)=K;  
Z=30;  
[K]=elev(Z,hc);  
O(31,:)=K;
```





APPENDIX C

MATLAB CODES FOR NUMERICAL SOLUTION

BASED ON RICHARDS EQUATION

C.1 The numerical simulation using Richards' equations for saline sand (Column II)

(Data for Figure 4.8)

```

% Implicit FD method to solve 1-D process-based Richards eqns
% (inverse method)
% Transient upflow in a soil column
% Boundary Condition
%h(z,0) = hinitial, L > z > 0 (start from water table to surface)
%h(0,0) = h0, (h minimum value)
%h(L,t) = hinitial, t > 0 (h minimum value)
%q(0,t) = q0, t > 0 (h maximum value)

h(0)=0; % h(0,0)=0
t(0)=0; % initial time
totaltime=t/24; % total time in days
dt=0.1/24; % time step (days)
maxstep=totaltime/dt; % max time steps
length=95; % soil column length (cm)
dz=1; % space step (cm)
n=round(length/dz)+1; % computing nodes
h2=-6; % Bottom pressure head (cm)
% ( minimum suction value)
h1=-1400; % Top pressure head (cm)
% ( maximum suction value)
q=0; % vertical flux (cm/day)(+ve for
% upward,-ve for downward)
Ks=150; % Saturated hydraulic conductivity
% Ks (cm/day)

% Coefficient of Tridiagonal nonlinear equation

a(1)=0;
b(1)=1;
c(1)=0;
a(n)=0;
b(n)=1;
c(n)=0;
d(1)=h1;
d(n)=h2;

for i=1:n
    u(i)=h1;
    pu(i)=h1;
end

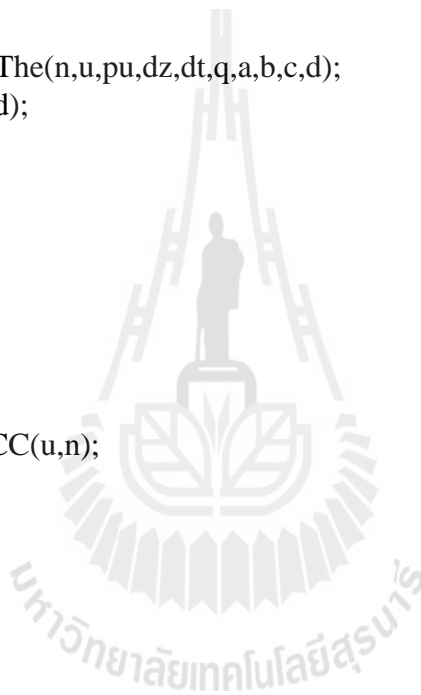
```

```
for i=1:n
    z(i)=dz*(i-1);
end

for i=1:n-1
    zz(n+1-i)=z(i);
end
zz(1)=z(n);

% Numerical Calculation for inverse method

for j=1:maxstep
    for i=1:5
        [a,b,c,d]=ChangeThe(n,u,pu,dz,dt,q,a,b,c,d);
        v=tridia2(n,a,b,c,d);
        for k=2:n
            u(k)=v(k);
        end
    end
    for i=2:n
        u(i)=v(i);
        pu(i)=u(i);
    end
    theta(j,:)=effsatSWCC(u,n);
    uu(j,:)=u;
end
```



```

% Plot final simulated results from reRICHARD.m
% Modeled the Unsaturated Upward Movement by Richard Equation (Sand)
% Ks=150 cm/d

axis([0 0.4 0 95]);

t=9;
reRICHARD;
orient landscape
set(gcf,'paperposition',[0 0 11 8.5]);

% Moisture content
plot(theta(2,:),zz,'m','linewidth',1.5);hold on % For t=0.25hr, j=2
plot(theta(90,:),zz,'b','linewidth',3.5);hold on% For t=9 hr, j=90
xlabel('Moisture Content (cm3 cm-3)','fontname','Times New Roman','fontsize',14);
ylabel('Height (cm)','fontname','Times New Roman','fontsize',14);

z1=[0 10 30 50 70 90];
the10=[0.37 0.2351 0 0 0 0];
the30=[0.37 0.2675 0.17 0 0 0];
plot(the10,z1,'m*-.','linewidth',2.0,'MarkerSize',8);hold on
plot(the30,z1,'b*-.','linewidth',1.0,'MarkerSize',12);hold on

% Label
text(0.15,70,'t = 15 mins','fontname','Times New Roman','fontsize',14);
text(0.2,80,'(Numerical)','fontname','Times New Roman','fontsize',14);
text(0.29,80,'(Experimental)','fontname','Times New Roman','fontsize',14);
plot([0.23 0.27],[70 70],'m','linewidth',1.5);
plot([0.32 0.36],[70 70],'m*-.','linewidth',2.0,'MarkerSize',8);
text(0.15,60,'t = 9 hrs','fontname','Times New Roman','fontsize',14);
plot([0.23 0.27],[60 60],'b','linewidth',3.5);
plot([0.32 0.36],[60 60],'b*-.','linewidth',1.0,'MarkerSize',12);
text(0.28,37,'ks = 150 cm/d','fontname','Times New Roman','fontsize',14);
text(0.22,29,'a = 0.02 (cm-1), b = 5','fontname','Times New Roman','fontsize',14);

```

% Function files (*.mfile) for inverse method

% (1) effsatSWCC.m file

```
function theta=effsatSWCC(u,n) % finding for theta (data from Maskong)
alpha=0.02; % a From Eq.(3.17) (cm-1)
h=5; % b From Eq.(3.17)
m=1-1/h; % c From Eq.(3.17)
tr=0.01;
ts=0.37;
for i=1:n
    top=(ts-tr);
    A=(alpha*(abs(u(i))))^h;
    C=1+A;
    bot=(C)^m;
    theta(i)=tr+top/bot; % Eq (3.17)
end
```

% (2) ChangeThe.m file

```
function [a,b,c,d]=ChangeThe(n,u,pu,dz,dt,q,a,b,c,d)
ca=TwP(u,n);
K=unsatHycond(u,n);
K(n+1)=K(n);
for i=2:n-1
    F1=ca(i)/dt;
    F2=(K(i)+K(i+1))/(2*dz^2);
    F3=-(K(i)+K(i-1))/(2*dz^2);
    F4=(K(i+1)-K(i-1))/(2*dz);
    a(i)=-F3;
    b(i)=-F2+F3-F1;
    c(i)=F2;
    d(i)=-F1*pu(i)-F4;
end
b(n)=b(n)+c(n);
Ka=(K(n)+K(n+1))/2;
d(n)=d(n)+c(n)*dz*(1+q/Ka);
c(n)=0;
```

% (3) TwP.m file (theta change with pressure change)

```
function ca=TwP(u,n)
% Empirical parameters (Let alpha=a,h=b,m=c) of van Genuchten
alpha=0.02; % a From Eq.(3.17) (cm-1)
h=5; % b From Eq.(3.17)
m=1-1/h; % c From Eq.(3.17)
tr=0.01; % data from Maskong(2010)
ts=0.37;
% Moisture capacity
for i=1:n
    top=(ts-tr);
    W=(alpha*(abs(u(i))))^h;
    D=1+W;
    bot=(D)^m;
    theta11=tr+top/bot; %  $\Theta$  in Eq (3.18)
    B=(alpha*(abs(u(i)+1)))^h;
    E=1+B;
    bot=(E)^m;
    theta22=tr+top/bot; %  $\Theta$  in Eq (3.18)
    ca(i)=(-theta11+theta22)/1; % theta change with pressure change
end
ca(1)=ca(2);
```

% (4) effsaturation.m file

```
function theta1=effsaturation(u,n) % theta *( $\Theta$ ) in Eq (3.18)
theta=effsatSWCC(u,n);
tr=0.01; % data from (data from Maskong)
ts=0.37;
for i=1:n
    top(i)=(theta(i)-tr);
    bot=(ts-tr);
    theta1(i)=top(i)/bot; %  $\Theta$  in Eq (3.18) (theta changes
    with pressure changes)
end
```

%(5) unsatHycond.m file

```
function [K]=unsatHycond(u,n) % data from (data from Maskong)
theta1=effsaturation(u,n); % theta *(Θ) in Eq (3.18)
h=5; % b From Eq.(3.17)
m=1-1/h; % c From Eq.(3.17)
Ks=150; % cm/d
for i=2:n
    K(i)=((theta1(i))^0.5)*(1-(1-(theta1(i))^(1/m))^m)^2; % Eq (3.18)
    if K(i)>1
        K(i)=1;
    else
        K(i)=K(i)*Ks;
    end
end
end
```

%(6) tridia2.m file (Tridiagonal coefficient matrix)

```
function [v]=tridia2(n,a,b,c,d)
bb=b;
dd=d;

for i=2:n
    ff=a(1,i)/bb(1,i-1);
    bb(1,i)=bb(1,i)-c(1,i-1)*ff;
    dd(1,i)=dd(1,i)-dd(1,i-1)*ff;
end
v(n)=dd(n)/bb(n);
for i=1:(n-1)
    j=n-i;
    v(1,j)=(dd(1,j)-c(1,j)*v(1,j+1))/bb(1,j);
end
```


C.2 The numerical simulation using Richards' equations for non saline sandy loam

(Data for Figure 4.10)

```

% Implicit FD method to solve 1-D process-based Richards eqns
% (inverse method)
% Transient upflow in a soil column
% Boundary Condition
%h(z,0) = hinitial, L > z > 0 (start from water table to surface)
%h(0,0) = h0, (h minimum value)
%h(L,t) = hinitial, t > 0 (h minimum value)
%q(0,t) = q0, t > 0 (h maximum value)

h(0)=0; % h(0,0)=0
t(0)=0; % initial time
totaltime=t/24; % total time in days
dt=0.1/24; % time step (days)
maxstep=totaltime/dt; % max time steps
length=95; % soil column length (cm)
dz=1; % space step (cm)
n=round(length/dz)+1; % computing nodes
h2=0; % Bottom pressure head (cm)
% ( minimum suction value)
h1=-1000; % Top pressure head (cm)
% ( maximum suction value)
q=0; % vertical flux (cm/day)(+ve for
% upward,-ve for downward)
Ks=3; % Saturated hydraulic conductivity
% Ks (cm/day)

% Coefficient of Tridiagonal nonlinear equation

a(1)=0;
b(1)=1;
c(1)=0;
a(n)=0;

```

```

b(n)=1;
c(n)=0;
d(1)=h1;
d(n)=h2;

for i=1:n
    u(i)=h1;
    pu(i)=h1;
end

for i=1:n
    z(i)=dz*(i-1);
end

for i=1:n-1
    zz(n+1-i)=z(i);
end
zz(1)=z(n);

% Numerical Calculation for inverse method

for j=1:maxstep
    t=j*dt;
    d(n)=-0-380*t/totaltime;
    for i=1:5
        [a,b,c,d]=ChangeThe(n,u,pu,dz,dt,q,a,b,c,d);
        v=tridia2(n,a,b,c,d);
        for k=2:n
            u(k)=v(k);
        end
    end
    for i=2:n
        u(i)=v(i);
        pu(i)=u(i);
    end
    theta(j,:)=effsatSWCC(u,n);
    uu(j,:)=u;
end

% Plot final simulated results from reRICHARD.m
% Modeled The Unsaturated Upward Movement by Richard Equation (non Saline
sandy loam)
% Ks=3 cm/d

```

```

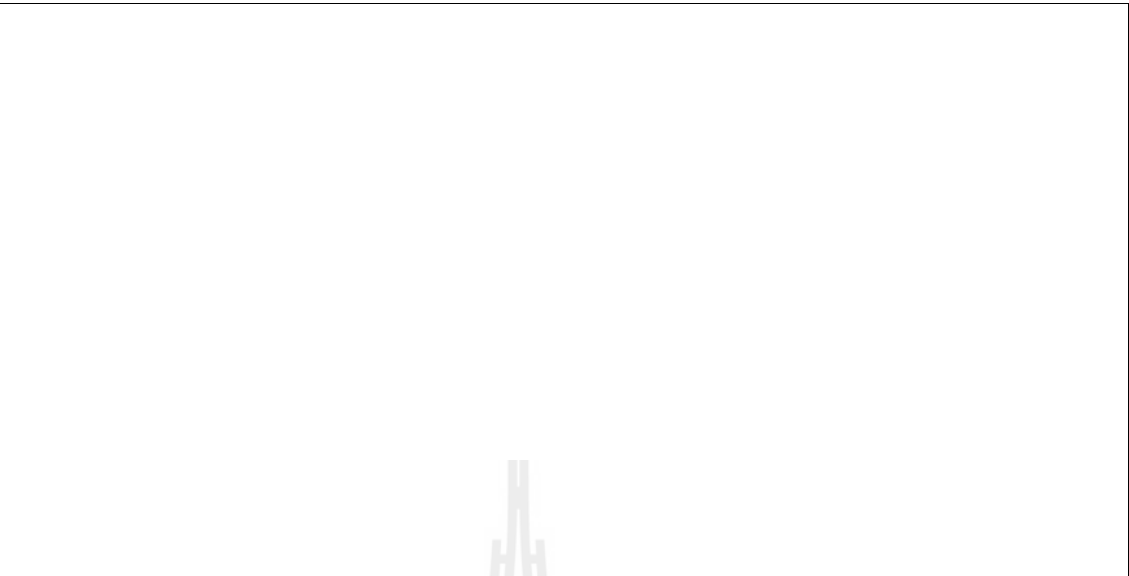
axis([0 0.45 0 95]);
t=216;
reRICHARD;
orient landscape
set(gcf,'paperposition',[0 0 11 8.5]);

% Moisture content
plot(theta(41,:),zz,'r','linewidth',1);hold on % For t=4.08hr, j=41
plot(theta(240,:),zz,'g','linewidth',2);hold on % For t=24 hr, j=240
plot(theta(1440,:),zz,'b','linewidth',2.5);hold on % For t=144hr, j=1440
plot(theta(2160,:),zz,'m','linewidth',3.5);hold on % For t=216 hr, j=2160
xlabel('Moisture Content (cm3 cm-3)','fontname','Times New Roman','fontsize',14);
ylabel('Height (cm)','fontname','Times New Roman','fontsize',14);

z1=[0 10 30 50 70 90];
the10=[0.36 0.32 0.072 0.062 0.065 0.058];% 4.08 hr
the30=[0.36 0.137 0.332 0.062 0.065 0.062];% 1day
the50=[0.36 0.142 0.146 0.201 0.069 0.06];% 6day
the70=[0.36 0.145 0.146 0.148 0.137 0.057];% 9day
plot(the10,z1,'r*-.','linewidth',1.0,'MarkerSize',8);hold on
plot(the30,z1,'g*-.','linewidth',1.5,'MarkerSize',10);hold on
plot(the50,z1,'b*-.','linewidth',2.0,'MarkerSize',12);hold on
plot(the70,z1,'m*-.','linewidth',2.5,'MarkerSize',13);hold on

% Label
text(0.25,70,'t = 4.08 hr','fontname','Times New Roman','fontsize',14);
text(0.3,80,'(Numerical)','fontname','Times New Roman','fontsize',14);
text(0.37,80,'(Experimental)','fontname','Times New Roman','fontsize',14);
plot([0.31 0.36],[70 70],'r','linewidth',1);
plot([0.38 0.42],[70 70],'r*-.','linewidth',1.0,'MarkerSize',8);
text(0.25,60,'t = 24 hrs','fontname','Times New Roman','fontsize',14);
plot([0.31 0.36],[60 60],'g','linewidth',2);
plot([0.38 0.42],[60 60],'g*-.','linewidth',1.5,'MarkerSize',10);
text(0.25,50,'t = 144 hrs','fontname','Times New Roman','fontsize',14);
plot([0.31 0.36],[50 50],'b','linewidth',2.5);
plot([0.38 0.42],[50 50],'b*-.','linewidth',2,'MarkerSize',12);
text(0.25,40,'t = 216 hrs','fontname','Times New Roman','fontsize',14);
plot([0.31 0.36],[40 40],'m','linewidth',3);
plot([0.38 0.42],[40 40],'m*-.','linewidth',2.5,'MarkerSize',13);
text(0.32,30,'ks = 3 cm/d','fontname','Times New Roman','fontsize',14);
text(0.28,22,'a = 0.01 (cm-1), b = 3.6','fontname','Times New Roman','fontsize',14);

```



C.3 The resulting wetting SWCC of the van Genuchten (1980) equations for saline sand (Column II) (Data for Figure 4.12(a))

```

% van Genuchten (1980) equation (Eq.(3.17))
% Sand
% Resulting SWCC (van Genuchten) from numerical solution

tr=1;           % (moisture content (%))
ts=37;         % (moisture content (%))
alpha=0.02;    % a From Eq.(3.17)
h=5;          % b From Eq.(3.17)
m=1-1/h;      % b From Eq.(3.17)
D=ones(1,10000);
Phi=1:10^4;
T=ones(1,10000);
T=tr*T;
for i=1:10000
a(i)=alpha*(Phi(i));
B(i)=a(i)^h;
end
for i=1:10000
C=(D+B);
F(i)=C(i)^m;
end
for i=1:10000
A=ts-tr;
S(i)=A/F(i);
end
for i=1:10000
Th=S+T;

```

```

end

z=0:1:n-2;
% Experimental data (Maskong, 2010)
z=0:1:n-2;
x=[0.00001 0.01 0.375];
y=[0.00001 10 30];
xx=[0.00001 0.01 0.375];
yy=[0.00001 10 32];

% Plotting for Experimental capillary rise

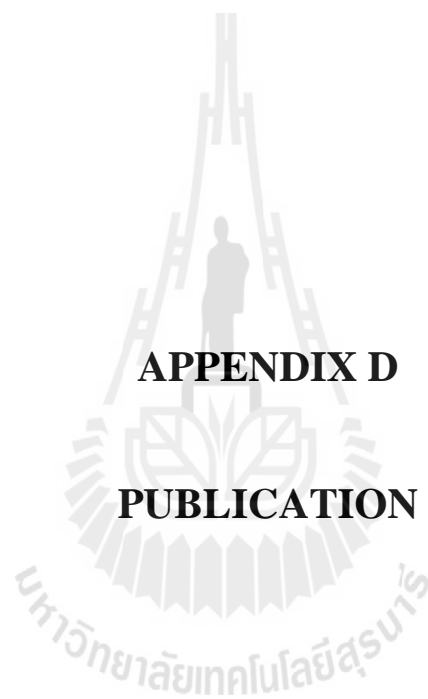
k=plot(x,y,'r*','linewidth',2.0,'MarkerSize',15);hold on

% Plotting for Simulated capillary rise (Numerical)
k=plot(xx,yy,'b*','linewidth',2.0,'MarkerSize',15);hold on

% Plotting for Simulated capillary rise (beta=1/ha)

k=plot(W,z,'m','linewidth',3.0);hold on
legend('Experimental capillary rise','Simulated capillary rise(Numerical)','Simulated
capillary rise(Analytical),  $\beta = 1/ha$ ','location','NorthWest');
set(gca,'Xscale','log','fontname','Times New Roman','fontsize',14);
set(gca,'Yscale','linear','fontname','Times New Roman','fontsize',14);
xlabel('Time (day)','fontname','Times New Roman','fontsize',14)
ylabel('Capillary Rise (cm)','fontname','Times New Roman','fontsize',14)
text(0.8,17,'ks = 150 cm/d','fontname','Times New Roman','fontsize',14);
text(0.8,13,'hc = 30cm','fontname','Times New Roman','fontsize',14);
text(0.8,9,'ha = 30cm','fontname','Times New Roman','fontsize',14);
text(0.8,5,'n = 0.37','fontname','Times New Roman','fontsize',14);
axis([0.00001 90 0 95]);

```



APPENDIX D

PUBLICATION

Publication

Htet Htet Aung., Jothityangkoon, C., and Maskong, H. (2013). **Estimation of the Rate of Capillary Rise in Sand and Sandy Loam based on One Dimensional Soil Column.** The Eighteenth National Convention on Civil Engineering, Chiang Mai, Thailand. WRE036, 4, pp. 98-102.





การประชุมวิชาการวิศวกรรมโยธาแห่งชาติ ครั้งที่ 18
18th National Convention on Civil Engineering



ประกาศนียบัตรรับรองการนำเสนอบทความ

ประกาศนียบัตรฉบับนี้ให้ไว้เพื่อแสดงว่า

Estimation of the Rate of Capillary Rise in Sand and Sandy Loam based on One
Dimensional Soil Column

Htet Htet Aung Chatchai Jothityangkoon and Haruetai Maskong

ได้นำเสนอ

ในงานการประชุมวิชาการวิศวกรรมโยธาแห่งชาติ ครั้งที่ 18

ระหว่างวันที่ 8-10 พฤษภาคม 2556

ณ โรงแรมดิเอ็มเพรส เชียงใหม่

(นายสุวัฒน์ เซาว์ปรีชา)

นายกวิศวกรรมสถานแห่งประเทศไทย

(รองศาสตราจารย์ นายแพทย์นิเวศน์ นันทจิต)

อธิการบดีมหาวิทยาลัยเชียงใหม่



การประชุมวิชาการวิศวกรรมโยธาแห่งชาติ ครั้งที่ 18
วันที่ 8-10 พฤษภาคม 2556 ณ โรงแรมดิเอ็มเพรส เชียงใหม่

Estimation of the Rate of Capillary Rise in Sand and Sandy Loam based on One Dimensional Soil Column

Htet Htet Aung¹, Chatchai Jothityangkoon² and Haruetai Maskong³

¹ Master Degree Graduate, ² Assistant Professor, ³ Doctoral Degree Graduate,

^{1,2,3} School of Civil Engineering, Institute of Engineering, Suranaree University of Technology,

Muang, Nakhon Ratchasima, 30000

E-mail: ¹ htethtet.aung22@gmail.com, ² cjothit@sut.ac.th, ³ haruetai.m@hotmail.com

Abstract

Soil salinity is one of the main environmental problems affecting extensive areas of land in both developed and developing countries. This salinity problem can be solved by capillary rise control of saline groundwater flow. The aim is to find a simple way to estimate the rate of capillary rise in the unsaturated soils using analytical solution. The maximum capillary heights of saline and non-saline soils (sand and sandy) are determined and compared with experimental results in one dimensional soil column. Sandy loam with saline water affects higher maximum capillary rise and higher soil moisture content than sandy loam with non-saline water, whereas, there is no difference for sand.

Keywords: unsaturated soils, salinity-affected area, analytical solutions

1. Introduction

The expansion of salinity-affected area in Northeast region of Thailand has been a serious environmental problem that cause to the decreasing of agricultural productivity and food production in this region. It is estimated that an area of 6 million hectares, or 34 percent of arable land, is already affected by salt [1]. Indications are that the problem is getting more widespread. A major cause of salt reaching the surface in this area is due to the rise of saline watertables to the capillary fringe and consequently the rise of salt to the surface [2]; [3]. Upward movement of these saline waters contributes to the salinisation of the area.

Capillary rise is the upward flux of water from the water table, which is driven by the capillary forces in the soil's pore spaces. At the water table the soil is saturated and water is at atmospheric pressure. The capillary pressure head (soil matric potential) is a function of soil moisture content, and increases as soil moisture decreases. If the soil

above the water table is not saturated, a soil matric potential gradient exists that induces an upward moisture flux from the water table. Three fundamental physical characteristics related to capillary rise are of primary practical concern: (1) the maximum height of capillary rise, (2) the fluid storage capacity of capillary rise, and (3) the rate of capillary rise.

This study proposes a model to estimate the rate of capillary rise using an analytical solution of Terzaghi's Equation. The required capillary data is gathered from the experimental results of [4]. In these experimental tests, the constant head water was introduced from the base of uniform soil column and there are two types of soil which are sand and sandy loam.

2. Theoretical Background

Terzaghi [5] formulated a simple theory based on Darcy's law and saturated hydraulic conductivity for predicting the rate of capillary rise in one - dimensional column of soil. To arrive at his solution for the rate of capillary rise, Terzaghi [5] made two major assumptions: (1) that Darcy's law for saturated fluid flow is roughly applicable to unsaturated flow, and (2) that the hydraulic gradient i responsible for capillary rise (i.e., hydraulic gradient of the wetting front located at the elevation z) can be approximated as follows;

$$i = \frac{h_c - z}{z} \quad (1)$$

where, h_c = the maximum height of capillary rise; and z = distance measured positive upward from the elevation of the water table [Fig. 1]. Physically, h_c represents the drop in pressure head across the air-water interface at the wetting front in the soil pores.

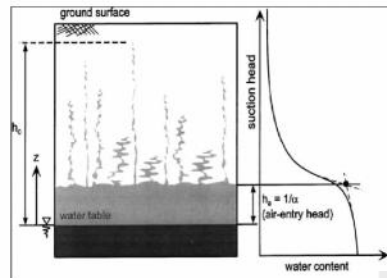


Fig. 1 Conceptual model for capillary rise and associated soil-water characteristic curve

Terzaghi's other assumption, Darcy's law is valid for capillary rise, can be expressed in familiar mathematical terms as follows;

$$q = K_s i = n \frac{dz}{dt} \tag{2}$$

where, q = discharge velocity; K_s and n are the saturated hydraulic conductivity and porosity of the soil, respectively.

Saturated hydraulic conductivity values are taken from Smedema and Rycroft's [6] ranges of K -values for certain soil textures (Table 1).

Solving Eqs. (1) and (2) and imposing an initial condition of zero capillary rise at zero time, Terzaghi arrived at the following solution describing the location of the capillary wetting front z as an implicit function of time;

$$t = \frac{nh_c}{K_s} \left(\ln \frac{h_c}{h_c - z} - \frac{z}{h_c} \right) \tag{3}$$

Fig. 1 shows a conceptual model for capillary rise and the associated relationship between suction head and water content, i.e., the soil-water characteristic curve. The soil profile is delineated by three distinct zones: a saturated zone located below the water table where the pore water pressure is positive, a saturated zone located below the air-entry head (h_a) but above the water table where the pore water pressure is negative with respect to atmospheric pressure, and an unsaturated zone located above the air-entry head where capillary water rises as a series of connected or disconnected fingers to maximum height h_c .

Table 1 Typical value of saturated hydraulic conductivity based on Texture and other soil properties

Soil properties	Order of magnitude of saturated hydraulic conductivity (m /day)
Coarse gravelly sand	10 - 50
Medium sand	1 - 5
Sandy loam/fine sand	1 - 3
Loam/clay loam/clay, well structured	0.5 - 2
Very fine sandy loam	0.2 - 0.5
Clay loam/clay, poorly structured	0.02 - 0.2
Dense clay, not cracked, no biopores	<0.002

The hydraulic conductivity of the unsaturated soil located above the air-entry head decreases dramatically as the pores begin to drain and the degree of saturation decreases with increasing rise. By the time the wetting front approaches h_c , the degree of saturation could be as low as a few percent and the hydraulic conductivity may be reduced by as much as 5-7 orders of magnitude its value at saturation. This significant reduction in hydraulic conductivity, together with the reduction in the available driving head ($h_c - z$), leads to a significant decrease in the rate of capillary rise as time progresses and the wetting front moves upward. Assuming that the hydraulic conductivity is a constant equal to the saturated conductivity is unrealistic, as Terzaghi [5] realized, and results in consequent over-prediction of the rate of capillary rise.

The characteristic dependence of hydraulic conductivity with respect to degree of saturation or suction in unsaturated soils has been a focus of intensive experimental and theoretical research since Terzaghi's original work. Numerous mathematical models for describing the unsaturated hydraulic conductivity function have been developed, the majority of which account for the drastic reduction in hydraulic conductivity with increasing suction using either exponential, power, or series functions.

[7] developed an alternative solution for the rate of capillary rise by incorporating Gardner's one-parameter exponential model [8] to estimate the unsaturated hydraulic conductivity function. Gardner's model [8] is expressed in terms of the saturated hydraulic conductivity K_s and suction head h_m as follows;

$$K(h_m) = K_s \exp(\beta x_m) \tag{4}$$

where, K is the unsaturated hydraulic conductivity at suction head h_m (cm) and β = a pore size distribution parameter (cm^{-1}) representing the rate of decrease in hydraulic conductivity with increasing suction head. The inverse of β has also been interpreted as the air-entry head, or equivalently, as the height of the saturated portion of the capillary fringe, i.e., $h_a = 1/\beta$.

Assuming Eq. (1) as the driving hydraulic gradient during capillary rise and Eq. (4) for the hydraulic conductivity at the wetting front z , the governing equation for one-dimensional capillary rise can be written as follows;

$$\frac{dz}{dt} = \frac{K_s}{n} \times \exp(-\beta z) \left(\frac{h_c - z}{z} \right) \quad (5)$$

Lu and Likos [9] contains the detailed solution to Eq. (5), which can be written in series form as follows;

$$t = \frac{n}{K_s} \sum_{j=0}^{m=\infty} \frac{\beta^j}{j!} \left[h_c^{j+1} \ln \frac{h_c}{h_c - z} - \sum_{s=0}^j \frac{h_c^s z^{j+1-s}}{j+1-s} \right] \quad (6)$$

If the nonlinearity in hydraulic conductivity is ignored by setting the series index m to zero, Equation (6) reduces to Terzaghi's original analytical solution Equation (3). Convergent solutions are typically obtained by setting m equal to 10.

The material parameter β can be determined if either the hydraulic conductivity function or soil-water characteristic curve are known or estimated. Given the former, β can be determined in conjunction with Gardner's model [8] to determine the "best fit" value. Given the latter, β can be determined using a graphical technique to estimate the air-entry head h_a and by recognizing that β may be interpreted as its inverse. The maximum height of capillary rise h_c may be approximated using a capillary tube analogy and applying the Young-Laplace equation to analyze mechanical equilibrium at the rising air/water interface. If both h_c and h_a are known, a dimensionless parameter βh_c equal to h_c/h_a . For the wide range of soil tested, the ratio h_c/h_a varies from 2 to 5 with only a few exceptions [7].

3. Results and Discussions

In order to examine the capillary rises, six uniform soil columns based on long column method from laboratory were studied. The long column method provided static

equilibrium volumetric water content at selected elevation along an upright column of soil [11].

Similar to experimental set up for the long soil column suggested by [11], each column was 95 cm in depth and water content probes were installed at 10, 30, 50, 70, 90 cm from the column base, as the desired matric head values. Constant head device was used to keep constant head of inflow water at 10 cm from the column base, presented in [4].

There were 2 types of soil sample (1) sand from sand pit at Pimai district Nakhon Ratchasima province, taking a sample with grain size passing sieve No.40 and retaining in sieve No.60, (2) sandy loam from Nong Khwao village, Non Thai district Nakhon Ratchasima province where facing soil salinity problem.

Two types of groundwater were used for these experiments: (1) deionized (non-saline) water represented deionized groundwater (DG) and (2) saline water prepared by dissolving pure NaCl with water until becoming saturated saline water, represented saline groundwater (SG).

The experiments four soil column are:

- (i) Column I : Sand and DG (Non-saline sand)
- (ii) Column II : Sand and SG (Saline sand)
- (iii) Column III: Sandy loam and DG (Non-saline sandy loam)
- (iv) Column IV: Sandy loam and SG (Saline sandy loam)
- (v) Column V : Sandy loam and SG adding artificial light
- (vi) Column VI: Sandy loam and SG adding moisture at the soil surface. The experiments were described fully in [4].

Table 2 shows the relation between capillary head and arrival time in sand soil column tests. For both SG and DG groundwater types in sand, the maximum capillary rise is 30 cm. The maximum capillary heights of sandy loam are 70 cm and 90 cm for the DG and SG types, respectively, that can be seen in Table 3.

The experimental measurements of the moving and maximum height of capillary rise varied with time were observed and extracted to present in Table 2 and 3. Porosity values of sand and sandy loam were 0.37 and 0.36, respectively, that are obtained from the direct measurement [4].

Table 2 The relation between capillary head and arrival time in sand soil column tests

capillary head (cm)	Column I		Column II	
	Moisture Content (%)	Arrival Time (day)	Moisture Content (%)	Arrival Time (day)
10	17.088	0.010	23.51	0.010
30	9.530	0.583	17.00	0.375
50	no change		no change	
70	no change		no change	
90	no change		no change	

Table 3(a) The relation between capillary head and arrival time in sandy loam soil column tests

capillary head (cm)	Column III		Column IV and V	
	Moisture Content (%)	Arrival Time (day)	Moisture Content (%)	Arrival Time (day)
10	32.0	0.17	34.0	0.13
30	33.2	1.00	33.2	1.00
50	20.1	6.00	31.9	4.00
70	13.7	9.00	30.5	7.00
90	no change		19.2	12.00

Table 3(b) The relation between capillary head and arrival time in sandy loam soil column test

capillary head (cm)	Column VI	
	Moisture Content (%)	Arrival Time (day)
10	36.1	0.17
30	no changes	
50	no changes	
70	no changes	
90	20.4	0.17

Fig. 2 shows the height of observed and simulated capillary rise as a function of time for Column I (non-saline sand) and Column II (saline sand). Comparison between experimental data and simulated data for the Column III (non-saline sandy loam) and Column IV (non-saline sandy loam) are shown in Fig. 3.

Rates of rise for these four soil columns were predicted using Lu and Likos's analytical solution Eq. (6). Direct measurement of h_w , K_s were not available for soils. Accordingly, βh_c for use in Eq. (6) was estimated in terms of "best fit" to the experimental data [4] for the soils.

For sand, seen in Fig. 2, the analytical solutions give a good fit to the experimental results at the beginning period, time is about 15 mins. At the longer time, the rate of capillary rise of simulated results tends to decrease and take longer time to arrive maximum rise at about 0.3 m.

The analytical solutions for both saline and non-saline sand are the same due to using the same βh_c . If βh_c is increased from 2 to 2.5, the rate of capillary rise will be decrease or spending more time to reach the maximum level (Fig. 4).

For sandy loam, shown in Fig. 3, simulated capillary rise from analytical solutions show a good agreement to the experimental capillary rise at a long time with the maximum capillary rise. However, analytical solutions give faster rate of capillary rise when moving capillary rise is less than maximum rise. With sensitivity analysis by increasing βh_c from 3.2 to 5, the analytical solutions show that the rate of capillary rise tend to decrease or take a longer time to arrive maximum rise (Fig. 5).

For the next step, a numerical solution of Richard's equation will be applied to simulate the rate of capillary rise.

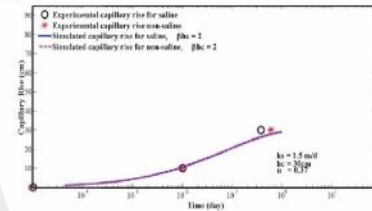


Fig. 2 The capillary rise vs. time for saline and non-saline sand comparison between E.R of [4] and A.S of [7] for $\beta h_c = 2$

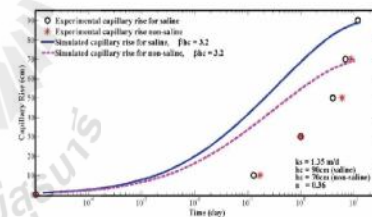


Fig. 3 The capillary rise vs. time for saline and non-saline sandy loam comparison between E.R of [4] and A.S of [7] for $\beta h_c = 3.2$

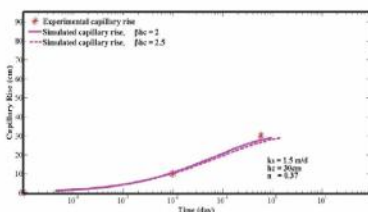


Fig. 4 The capillary rise vs. time for non-saline sand comparison between E.R of [4] and A.S of [7] using $\beta h_c = 2$ and 2.5

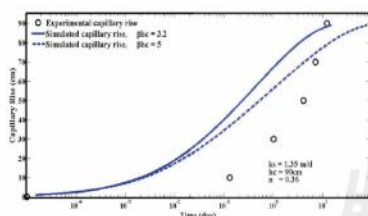


Fig. 5 The capillary rise vs. time for saline sandy loam comparison between E.R of [4] and A.S of [7] using $\beta h_c = 3.2$ and 5
 Notes: E.R is experimental results and A.S is analytical solutions

4. Conclusion

The maximum capillary rises of saline and non-saline sand are the same, showing in both experiments and simulation with analytical method. Analytical model is able to estimate the rate of capillary rise close to experimental results. For sandy loam, saline water affects higher maximum capillary rise, higher rate of capillary rise and higher soil moisture content than non-saline water. Simulated results using analytical model show that the rate of capillary rise is sensitive to dimensionless parameter βh_c . The increase of βh_c values results the decrease of the rate of capillary rise and provide over-estimate time to maximum capillary rise. The solutions may be used to solve the engineering problems involving time dependent wetting processes resulting from capillary rise, whereas it's suitable for the short durations and capillary rise in shallow groundwater.

5. Acknowledgement

The first author would like to thank to Thailand International Development Cooperation Agency (TICA), Royal Thai Government for awarding her scholarship.

References

- [1] F. Ghassemi, A.J. Jakeman and H.A. Nix. *Salinisation of Land and Water Resources: Human Causes, Extent, Management and Case Studies*. Oxford, CAB International, 1995.
- [2] S. Konyai, V. Sriboonlue and V. Trelo-ges. "The Effect of Air Entry Values on Hysteresis of Water Retention Curve in Saline Soil." *American Journal of Environmental Sciences*, 5, pp. 341-345, 2009.
- [3] E. Löffler and J. Kubiniok. "Soil salinization in north-east Thailand." *Erkundung*, 42, pp. 89-100, February, 1988.
- [4] H. Maskong. "Capillary cut for salinity control in sandy loam." M. thesis, School of Civil Engineering, Suranaree University of Technology, Nakhonrachasima, Thailand, 2010.
- [5] K. Terzaghi. *Theoretical Soil Mechanics*. New York: Wiley, 1943.
- [6] L.K. Smedema and D.W. Rycroft. *Land drainage : planning and design of Agricultural Drainage Systems*. Batsford, London, pp.376, 1983.
- [7] N. Lu and W.J. Likos. *Unsaturated Soil Mechanics*. New Jersey: Wiley, 2004.
- [8] W.R. Gardner. "Some steady state solutions of the unsaturated moisture flow equation with application to evaporation from a water table." *Soil Science*, 85, No.4, pp. 228-232, 1958.
- [9] N. Lu and W.J. Likos. "Rate of capillary rise in soil." *Journal of the Geotechnical and Geoenvironmental Engineering*, 130, No. 6, pp. 649-650, June, 2004.
- [10] J.J. Douglas and B.F. Jones. "On Predictor-Corrector Method for Non-Linear Parabolic Differential Equations." *Journal of the Society for Industrial & Applied Mathematics*, 11, No.1, pp. 195-204, 1963.
- [11] W.D. Reynolds and G.C. Topp. "Soil water desorption and imbibition: tension and pressure techniques." *Soil sampling and methods of analysis*, 2nd ed. CRC Press, Boca Raton, FL, pp. 981-998, 2008.

BIOGRAPHY

Mrs. Htet Htet Aung was born on January 12, 1980 in Yangon, Myanmar. She received her bachelor's degree in Civil Engineering from Yangon Technological University Myanmar in 2005. She has worked as an engineer in River Engineering department at Directorate of Water Resources and Improvement of River Systems, Myanmar since 2005. In 2011, she received a ACMECS Master's degree scholarship to pursue M.Eng study in Civil Engineering at Suranaree University of Technology (SUT) from the Thailand International Development Cooperation Agency (TICA), Ministry of Foreign Affairs of Thailand. She enrolled in the Master's degree program in the school of Civil Engineering at SUT and obtained her degree in Civil Engineering in 2013. During her M.Eng study, she published 1-international conference paper.

